



SAPIENZA  
UNIVERSITÀ DI ROMA

Dipartimento di Fisiologia e Farmacologia

PhD Program in Neurophysiology

XXV cycle

The role of Parietal Cortex in the Online Control of  
Hand Movement Trajectory:  
an Inactivation and a Case Report Study

Simone Ferrari-Toniolo

*Supervisor:* Prof. Alexandra Battaglia-Mayer

*PhD Coordinator:* Prof. Roberto Caminiti

PhD Dissertation

February 2013

# INDEX

ABSTRACT	3
INTRODUCTION	5
- Hand reaching movements	5
- The cortical network for visual reaching	6
- The on-line control of movement	7
- The parietal syndrome	8
- Aim of the present study	9
SECTION 1	10
IMPAIRMENT OF ONLINE CONTROL OF HAND AND EYE MOVEMENTS IN A MONKEY MODEL OF OPTIC ATAXIA	
- Introduction	11
- Methods	13
- Results	21
- Discussion	35
SECTION 2	40
OPTIC ATAXIA GENERALIZES TO HAND MOVEMENT UNDER ISOMETRIC CONDITIONS	
- Introduction	41
- Methods	43
- Results	49
- Discussion	58
REFERENCES	61

## ABSTRACT

The role of the Superior Parietal Lobule (SPL) of the primate brain in the control of hand and eye movements has been investigated through two experiments. In one experiment two macaque monkeys were trained to perform arm movements under two task conditions. In the first the animal performed direct reaches from a central location to one of 4 peripheral visual targets. In a second condition (50% of the trials) a sudden change of target location occurred, either during the hand reaction-time (RT) or at movement-time (MT) onset. The animals were required to adjust as fast as possible their hand trajectory to reach the second target location. A behavioral testing was performed before and after SPL inactivation. The inactivated area had previously been studied in the same task by recording the activity of 225 cells that showed modulation by hand position, speed and movement direction, as well as by saccadic signals. In separate sessions, unilateral and bilateral injections of the GABA-A agonist muscimol were performed within area 5 (PE/PEc) of the SPL. As control, physiological saline was injected in the same loci. Bilateral muscimol injections caused an increase of the hand RT and MT toward the first target in the direct reaches, and to both the first and second target in the corrected ones. In the latter, this resulted in an increase of the time necessary for the correction of the hand trajectory and in an elongation of the hand-path toward the first target location. During corrected reaches, an elongation of the eye RT to both first and second target was also observed, together with a change of eye-hand coupling, which could partially explain the hand reaching disorder. These results identify SPL as a crucial node in the on-line control of hand and eye movement, and highlight the role of an eye impairment in the emergence of the movement disorder characteristic of Optic Ataxia (OA).

In a second experiment a patient with OA from unilateral tumor lesion of the right SPL and a group of 8 age-matched normal control subjects were asked to perform reaching movements from a central position to peripheral visual targets presented on a touch-screen. The subjects were also requested to perform a similar center-out task under isometric condition, where a force had to be applied to an isometric manipulandum in order to move a visual cursor from the center of the workspace to peripheral visual targets. Both tasks were

performed with and without central fixation (extrafoveal and foveal condition, respectively). The results show no major impairments in the temporal aspects of the movement (such as eye and hand RT and MT). On the contrary, in the extrafoveal condition the patient showed larger constant errors (CE) of the movement endpoints than controls in both the reaching and isometric task. In the foveal condition statistically higher CEs were observed only in the isometric task. The patient also showed a higher variability in the endpoints' position as compared to controls across all tested conditions. These results show that OA can emerge not only when a hand movement is performed, but also when only a force pulse of desired strength and direction has to be generated.

# INTRODUCTION

## **Hand reaching movements**

Hand reaching movements are central to many human activities including eating, tool use, work, and sports, becoming a defining characteristic typical of human life. As a consequence, an impairment of this ability following disease, stroke, injury or developmental disorders, results in a considerable deterioration in the quality of life and productivity.

A common type of reaching movements is the so-called visual reaching, in which a visible object is the final target of a hand movement. To perform a visual reaching it is necessary to identify the spatial location to be reached and transform the target location from retinal to body-centred coordinates to generate a spatio-temporal pattern of muscle r contractions adequate to bring the hand to the target.

Therefore, to plan a visual reaching the central nervous system must transform the pattern of retinal stimulation caused by the object into the correct sequence of muscles activity. This transformation implies a remapping of the target location from the initial retinotopic coordinates to body- or hand-centered frames of reference (Battaglia-Mayer et al., 2003). The remapping depends on the combination of retinal and extra-retinal neural signals with somatic information coding the position of body segments, to compute hand and target's relative positions. This set of operations must be carried on continuously for the whole duration of the reaching movement, during which the arm, eye, head and trunk move.

To achieve optimal performance in reaching movements, gaze and arm movements have to be precisely coordinated: the eye normally attains the target well before the hand and stays there until the hand reach is completed.

Eye and arm control systems could be fed by a common input drive, or one of these two systems could be the master and the other one could be the slave (Carey, 2000). Either way a coordination between eye and hand movements is needed to achieve the best performance in reaching, and some neural mechanism

has to be responsible for a fine tuning of this coordinated action.

### **The cortical network for visual reaching**

Neurophysiological studies on monkey models made it possible to identify the main neural substrates responsible for the coordinated mechanisms underlying visual reaching. The control of reaching movements is mediated by a distributed cortical system that includes populations of neurons from different parietal and frontal cortical areas. These are linked by cortico-cortical connections that are always reciprocal, implying that the functional mechanisms of each area are not independent from the mechanisms of the other areas involved in the network. Therefore it is not possible to univocally link a given physiological function to any given area. It has also been shown that individual neurons of this network combine and encode different visuo-motor signals and parameters (Battaglia-Mayer et al., 2003). Nonetheless it is possible to identify some characteristics specific to each area of the network.

The primary motor cortex (M1) is the last cortical stage of integration of the motor command, containing populations of neurons encoding the correct force and direction for the execution of hand reaching movements. The premotor cortex (PM) integrates the signals coming from the parietal cortex, the prefrontal cortex and other sub-cortical areas, to select and generate the appropriate motor command for the requested task.

The posterior parietal cortex (PPC), a high-order association area, plays a critical role in integrating visual and somatic signals, as it receives inputs both from the visual and somatosensory areas. Being reciprocally connected to the cortical output-areas of the frontal lobe, namely the premotor and motor cortices, it can be considered as an early and intermediate stage in the processes leading from vision to action.

The PPC integrates multimodal sensory and motor signals to process spatial information for a variety of functions, including attention, decision making, action understanding, and movement planning (Kalaska et al., 1997; Gold and Shadlen, 2007; Bisley and Goldberg, 2010; Fogassi et al., 2005). The combination of

signals in PPC is not limited to information of different modalities, but also refers to signals related to different effectors, such as the eye and the hand (Battaglia-Mayer et al., 2000, 2001, Marconi et al. 2001). For this reason it has been suggested that PPC plays a crucial role in the early stages of eye–hand coordination necessary for any successful reach, under a variety of experimental conditions (Mascaro et al., 2003, Battaglia-Mayer et al., 2003, 2006).

In conclusion, the pattern of cortico-cortical connections in the parieto-frontal network defines a gradient of visual, eye, and hand information critical for localizing target objects and for reaching toward them.

### **The on-line control of movement**

If the location of a target object suddenly changes during planning or execution of a reaching movement the brain has to re-compute the movement parameters necessary to reach for the new location. A key feature of the primates' motor behavior is the ability to make fast *on-line* corrections of hand movement trajectories after such changes (Archambault et al., 2009). Psychophysical studies have shown that the time needed for an on-line reaction to a target change can be as low as 100ms, resulting in the ability, given enough time for correction, to reach for the new target without completing the movement planned toward the first one. These results suggest that the nervous system continuously monitors ongoing movements, and can modify them at any time, if requested by a change in the environment.

Only few studies have analyzed the neural mechanisms underlying this behaviour. In the primary motor cortex (Georgopoulos et al., 1983; Archambault et al., 2011), the pattern of neuronal activity related to hand movement to a first target is truncated upon presentation of a second one, and is replaced by a pattern of activity similar to that observed during movement from the starting point to this new target. Several lines of evidence identify the PPC as a crucial node in the process of updating hand movement trajectory. A study of PPC (Archambault et al., 2009, 2011) confirmed this hypothesis, by showing a strong correlation between parietal neural activity and hand movement parameters such as speed, direction and

position, all necessary for online control of hand trajectory. In particular, parietal cells were found to modulate their firing frequency in a way that preceded the change in hand trajectory after the change in target location. Other parietal neurons were also found to change their activity after the correction of the movement, suggesting that in PPC predictive signals coexist with feedback information concerning ongoing movement.

### **The parietal syndrome**

These results are in agreement with observations on human patients. Lesions of the PPC in humans can lead to complex syndrome, originally described by Balint (1909) and consisting of an inability to perceive and react to stimuli in the visual space contralateral to the lesion (hemispatial neglect), an inability to voluntarily control gaze and move the focus of visual attention (gaze apraxia), and difficulty to coordinate hand movements to visual targets (Caminiti et al., 2010; Battaglia-Mayer and Caminiti, 2002; Buxbaum et al., 2004; Hécaen and de Ajuriaguerra 1954; De Renzi, 1982), the latter being a condition known as optic ataxia (OA). OA can occur independently of the other parietal symptoms and can be dissociated from motor, somatosensory, visual acuity, or visual field deficits (Perenin and Vighetto, 1988; Rossetti et al., 2003).

In a pioneering study Perenin and Vighetto (Perenin and Vighetto, 1988) analyzed the performance of stroke patients with parietal lesions while they were performed a simple reaching task. Patients with unilateral lesion were found to be more inaccurate when reaching towards their contralesional visual field, independently of the hand used. As confirmed by successive studies, this pattern is observed when testing subjects in extra-foveal condition, that is when the stimuli to be reached are presented in periphery of the visual field.

A case report of an optic ataxic patient with bilateral PPC lesion tested under a different experimental condition showed an additional and intriguing deficit. The patient showed a marked difficulty in producing smooth corrections of hand trajectory following a target jump, while reaching to stationary targets remained unaffected (Pisella et al., 2000; Grea et al., 2002). This result conforms to previous studies performed on



humans by perturbing the PPC activity through transcranial magnetic stimulation (Desmurget et al. 1999; Johnson and Haggard 2005).

In conclusion, two types of impairments are observed in association to optic ataxic patients, namely misreaching toward targets in the periphery and an inability to make fast online movement corrections.

### **Aim of the present study**

The present work is aimed at finding a causal relationship between the neural activity of the parietal cortex and the observed motor behaviour. This goal is pursued by investigating the role of PPC in the emergence of OA deficits by means of two different experiments: an inactivation study on a monkey model of OA and a case report on a parietal patient with OA.

The present manuscript is therefore divided into two main sections:

*Section 1* contains the analysis and the discussion of the first experiment, which has been published on *Cerebral Cortex* (Battaglia-mayer et al., 2012). This inactivation study was carried out on monkeys while they performed a reaching task requiring online corrections of hand movement trajectory. The aim of the experiment was to test the hypothesis that controlled lesions of the monkey PPC would produce OA-like symptoms, resulting in an impairment of the ability to adjust hand reaches during their execution. This would show the existence of a causal relationship between PPC neural activity and the on-line control of reaching.

*Section 2* contains the analysis of the data from the second experiment. In this study a patient with OA from unilateral tumor lesion of the right PPC and a group of 8 age-matched normal control subjects were asked to perform reaching movements from a central position to peripheral visual targets presented on a touch-screen. In a second task, subjects were also requested to perform a similar center-out task under isometric condition, where a force had to be applied to an isometric joystick in order to guide a visual cursor from the center of the workspace to different peripheral targets. The aim of this experiment was to test the hypothesis that OA symptoms also arise for movement under isometric conditions, where no hand or arm displacement is requested.

## SECTION 1

### **Impairment of online control of hand and eye movements in a monkey model of optic ataxia**

Publication reference:

Battaglia-Mayer A, **Ferrari-Toniolo S**, Visco-Comandini F, Archambault P S, Saberi-Moghadam S, Caminiti R. 2012. Impairment of Online Control of Hand and Eye Movements in a Monkey Model of Optic Ataxia. *Cereb Cortex* (online, doi:10.1093/cercor/bhs250)

## INTRODUCTION

On-line control of movement allows changing motor plan, as required for fast corrections of the hand trajectory, when the target moves in space. When enough time is allowed for correction, human subjects and monkeys will not complete hand movement to the first target's location, but will produce a curved trajectory toward the final one (Carlton, 1981; Georgopoulos et al. 1981; Georgopoulos et al. 1983; Soechting and Lacquaniti 1983; Archambault et al. 2009). Movement can be adjusted without awareness of the target's shift, i.e. during saccades (Blouin et al. 1995), in the absence of visual feed-back about arm movement (Pelisson et al. 1986), as well as by de-afferented patients devoid of limb proprioception (Bard et al. 1999; Sarlegna et al. 2006). On-line corrections might reside on motor outflow (Desmurget and Grafton 2000), and/or on sensory information, such as retinal error (Blouin et al. 1995; Desmurget et al. 1999).

Although rather resistant to peripheral lesions or to lack of peripheral information, on-line hand correction is severely affected by central lesions, such as those involving the posterior parietal cortex (PPC). A case report of Optic Ataxia (OA) from bilateral PPC lesion has shown a marked difficulty to produce smooth corrections of hand trajectory, while reaching to stationary targets remained unaffected (Pisella et al. 2000; Grea et al. 2002). This result conforms to previous studies performed in humans by perturbing the PPC activity through transcranial magnetic stimulation (Desmurget et al. 1999; Johnson and Haggard 2005). Recent studies in behaving monkeys have revealed a differential role of premotor, motor, and posterior parietal cortex (Archambault et al. 2009; 2011; see also Georgopoulos et al. 1983) in signaling the change of target location and implementing the hand trajectory correction. These studies were of correlative nature, therefore did not allow determining a causal relationship between parietal neural activity and on-line control of hand trajectory.

In the present study we explored whether the inactivation of the Superior Parietal Lobule (SPL) in monkeys leads to difficulties in producing smooth on-line corrections of hand movement in response to a shift in target location. We also studied the potential contribution of concurrent eye deficits to the difficulty

of adjustment of hand trajectory. We first characterized the functional properties of parietal cells, by recording neural activity in monkeys performing direct as well as corrected reaches. Then, the region of recording was reversibly silenced by injecting the GABA-A agonist muscimol , and the animal behavior was reassessed under such condition. A constellation of deficits affected both the spatial and temporal aspects of on-line control of hand movement trajectory, of eye movement, and of eye-hand coupling.

These results are relevant for the identification of the parietal region responsible for the deficits observed in humans, since so far these deficits have only been described in a case report of a patient with a large, bilateral occipito-parietal lesion, which does not provide a precise localization of the relevant critical region. They also relate to the elucidation of the eye contribution to the hand reach disorder typical of OA.

## METHODS

### *Animals*

Two male *Macaca mulatta* monkeys (body weights 5.2 and 6.0 kg) were used in the study, in accordance with the European (Directive 86/609 EEC) and the Italian (D.L. 116/92) laws on the use of animals in scientific procedures.

### *Behavioral tasks*

*Reaching tasks.* The monkeys performed arm reaches to visual targets in 3D space under two conditions (**Fig. 1A, B**):

1. *Direct reach.* In this conditions the animal was required to make direct reaches from a central push-button to one of eight peripheral visual targets, consisting of push buttons that were presented by two robotic arms at the vertices of a virtual cube and in total darkness. When the central button was turned green, the monkey was required to press and fixate that button for a variable control time (800-1500 ms; CT; **Fig. 1B**), at the end of which a red peripheral target was lit and the animal was required to reach and press it for a variable target holding time (500-1000 ms; THT; **Fig. 1B**).

2. *Corrected reach.* In 50% of the trials, the position of the peripheral target changed, either during reaction-time (160 ms after the presentation of the first target, **Fig. 1A-center**), or at the onset of hand movement (**Fig. 1B**), by turning off the target on one robotic arm and lighting the target on the second one. The target “jumped” from its original position either to the opposite vertex of the cube (at 180°; **Fig. 1A right**) or to one adjacent (at 90°) and immediately to the left (for right targets), and vice-versa for left targets. Therefore, there were four corrected conditions characterized by two switching times and two switching directions. The animal was required to update the original movement plan or the ongoing movement and reach toward the second target.

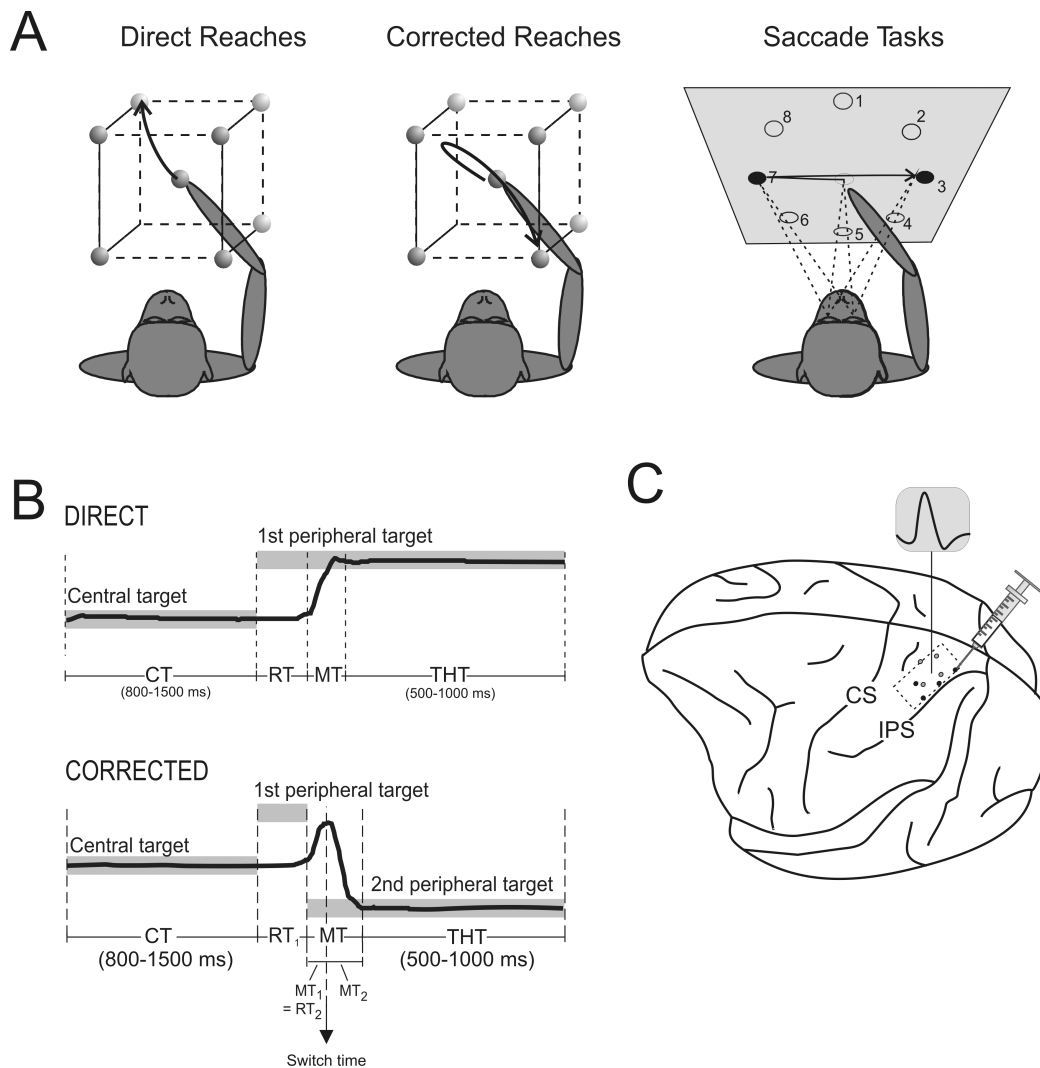


**Figure 1.** (A) Experimental apparatus. Monkeys performed *direct* (left) or *corrected* reaches (centre), in total darkness, starting from a central position to one of the 8 peripheral targets, placed at the vertices of an imaginary cube. A similar apparatus was used for the Saccade tasks (right), in absence of hand movements. In this example the target moves from position 7 to 3 (B) Temporal sequence and duration of events during *direct* and *corrected* reaches: CT, RT, MT, THT refer in order to control time, reaction-time, movement-time, target holding time. RT<sub>1</sub> is the hand reaction-time to the first target, MT<sub>1</sub> and MT<sub>2</sub> refer to hand movement-time to the first and second target, respectively; the “Switch time” refers to the moment in which the hand deviates from its initial trajectory. Gray bars represent the intervals of visual targets presentation, at different locations. Correspondingly, black lines indicate the evolution in time of one coordinate of the hand position. (C) Region of electrophysiological recordings (rectangle) and entry points of muscimol injections in monkey 1 (gray) and monkey 2 (black), in areas PE/PEc of the Superior Parietal Lobule (Brodmann area 5), superimposed on a common brain figurine. Same patterns of injections were adopted in the opposite hemisphere (not shown). CS and IPS indicate central and intraparietal sulci.

*Saccade tasks.* Two types of saccade tasks (**Fig. 1A, right**) were used to identifying the influence of eye-related signals on neural activity recorded in the reaching tasks, as well as potential deficits of eye movement after muscimol injections:

1. *Single-step saccade.* The monkey fixated (and pressed) a central button for a variable control time (CT, 800-1500 ms). Then, one of eight peripheral targets was presented at 45° angular intervals on a circle of 18° visual field radius. The monkey was required to make a saccade to the target and keep fixation there for 500 ms.

2. *Double-step Saccade.* In 50% of the trials the peripheral target was turned off during eye reaction time (150 ms after the presentation of the first peripheral target), and replaced by the opposite one at 180° in the circle.

Details on the tasks used for physiological recordings are given in Archambault et al 2009.

The monkeys performed the same tasks after muscimol injection (see below). However, because of the limited duration of the muscimol effect, instead of 8 possible movement targets we used only the four front targets of the workspace, those closer to the animal. Corrected reaches were only made for the 180° target jump, either during reaction-time or at the onset of movement-time. This led to a total of 4 movement directions for direct reaches and single-step saccade trials, to 8 movement conditions (4 directions X 2 switch times) for the corrected reaches, and to 8 conditions for the double –step saccades. Before and after muscimol injection, each hand or eye movement condition was repeated for at least 10 replications, for a total of 80 trials. To ensure a one-to-one ratio between the occurrence of direct and corrected movements, the former were presented two times as frequently (20 replications for each of the 4 direction) for a total of 80 trials. In both the muscimol and the control trials, all conditions were pseudo-randomized and presented in an intermingled design. Successful trials were rewarded with apple juice or water.

### *Muscimol injection*

Each animal was first used for neurophysiological recording for about 3 months. Once this was

completed, the inactivation experiment was performed in different sessions. The GABA-A agonist muscimol (Sigma Aldrich) was dissolved in sterile physiological saline (5 g/ l) and injected through a micro syringe. In each day, the session consisted of testing the effects of parietal inactivation on both the reaching and saccade tasks. In separated sessions, cortical inactivation was performed unilaterally (UL-I) in the left and right hemisphere, or bilaterally (BL-I), as shown in Table 1.

**TABLE 1**  
Schematic representation of experimental protocol

Session 1	Session 2	Session 3	Session 4
day 1	day 3	day 5	day 7
<i>Behavioral Testing (hand and saccade tasks), before injection</i>			
<b>(Control No-I)</b>			
Muscimol Injection	Muscimol Injection	Muscimol Injection	Saline Injection
<b>Unilateral Right (UL-I)</b>	<b>Bilateral (BL-I)</b>	<b>Unilateral Left (UL-I)</b>	<b>Bilateral SAL-I</b>
Rest (2 hours)			
<i>Behavioral Testing (hand and saccade tasks), after injection</i>			

At the beginning of each day, the session started by testing the normal animal's behavior before the muscimol injection, as control. Then, injections (*unilateral or bilateral*) were made. After 2 hours rest, the animal were re-tested. In each hemisphere, four injections (1 µl, each), spaced 1 mm apart, were made into the region of physiological recording in the SPL (**Fig. 1**), or in the homologous region of the other hemisphere. In all cases, the consequences of unilateral and bilateral inactivation were tested on both arms. As a further control, experimental sessions similar to those described above (i.e. behaviour → injections → behaviour) were repeated, by making 4 injections of sterile physiological saline (SAL-I; 1 µl, each) in the same cortical region/s, as to exclude that the observed effects of muscimol were due to local oedema or to dilution of the extracellular matrix.



### *Behavioral control*

Custom-made software controlled the movement of the robots, the switching of the lights and recorded the time of button press and release. Arm position was recorded in 3-D using an opto-electronic system (Optotrak, Northern Digital, Waterloo, Canada) and sampled at 100 Hz. Six markers were attached to a tight-fitting sleeve on the monkey's forearm to reconstruct hand trajectories. Eye position signals were recorded by using an implanted scleral search coil (1° resolution) and sampled at 200 Hz (Rommel Labs, Ashland, MA). Fixation accuracy was controlled through circular windows (5° diameter) around the targets.

During recording, an upper limit was placed on the hand reaction-time as the mean reaction-time plus one standard deviation of all the trials recorded during the last two weeks of training. For the eye task, reaction and movement-time together had to be less than 400 ms.

### *Neural recording*

The activity of single neurons was recorded with extra-cellular electrodes, using a 7-channel array (Thomas Recording GmbH, Giessen, Germany). Electrodes were glass-coated tungsten-platinum fibers ( 1-2 MΩ impedance at 1 kHz).

### *Data analysis*

*Behavioral epochs.* The time of change in the direction of hand movement during corrected reaches was determined by first calculating the mean and confidence interval of the hand trajectory in the  $x$ ,  $y$ ,  $z$  coordinates, over all direct reaches to each of the targets. The 95% confidence interval was obtained using the bootstrap statistics. The instant of change of movement trajectory (*Switch Time*) was then calculated by comparing each corrected reach trajectory with the mean direct reach movement to the same target. This time was defined as the first of a series of three points exiting its confidence interval in any of the  $x$ ,  $y$  or  $z$  coordinates.

For the eye, the angular velocity was first derived from the position signal. The onset and offset of the saccade was taken as the first of a sequence of three points exceeding or falling below a threshold of 50°/sec, respectively. There was no need to calculate a switch time for the double-step conditions, as the eye always completed the saccade to the first target before moving to the second one.

With these values, we could define various epochs describing the animal's behavior (**Fig. 1B**). In the *Direct reach* task, the CT ended with the presentation of the first target and the RT was defined as the time elapsing from the presentation of the target to the onset of hand movement. Only one period of hand movement (MT) was detectable in this task condition. In the *Corrected reach* task (**Fig. 1B**), two RTs were defined, RT<sub>1</sub> as the interval from the presentation of the first target to the onset of hand movement, RT<sub>2</sub> elapsing from the second stimulus onset to the change of hand movement direction, as determined by the instant of hand trajectory switch (**Fig. 1B**). In this task, the MT could be divided in two distinct epochs, based on the time the hand traveled toward the first (MT<sub>1</sub>) and second (MT<sub>2</sub>) target. For the *Single-step Saccade* task, the division into behavioral epochs was similar to that of the *Reaching* task. In the *Double-step Saccade* task we defined two periods for eye RT and MT (RT<sub>1</sub> and MT<sub>1</sub> followed by RT<sub>2</sub> and MT<sub>2</sub>).

Appropriate statistical tools, such as ANOVA ( $p < 0.01$ ) or Kolmogorov-Smirnov (K-S) test ( $p < 0.01$ ) were used to assess differences in the task performance after muscimol and saline injection, relative to control.

*Neural data.* A 2-way ANOVA (factor 1: epoch, factor 2: target position) was used to study the modulation of neural activity in different epochs of the tasks. In the reaching tasks we compared the mean spike frequency of *Direct reach* trials, collected during RT, MT and THT to the one recorded during CT. In the Saccade task the comparison was performed between mean spike frequency of *Single-step trials* in RMT (RT+MT) and THT with the corresponding CT. A cell was defined as being modulated in a given epoch if factor 1 or the interaction term was significant ( $p < 0.05$ ). A cell classification was also attempted to identify the main influence on cell activation between hand movement (reaching) and saccade behavior. Cells were classified as hand-dominant, eye-dominant or eye-hand related on the basis of ad hoc modulation indices

(see Archambault et al. 2009). The available kinematics data were used to calculate the length in time of the different behavioral epochs and the time of switch of hand trajectory in the corrected reaches trials. To examine hand dominant-cells in more details, the relationships between their neural activity and the hand's kinematics during both direct and corrected reaches were modeled through a multiple linear regression (Archambault et al. 2009).

*Reconstruction of hand trajectory.* The relationship between hand position and the six markers placed on the monkey's forearm was calculated using a known reference point, i.e., the hand's resting position on a fixed peripheral target at the end of movement. We adopted an algorithm based on singular value decomposition, which makes use of the redundant information, in the least-square sense (Soderkvist and Wedin 1993). This method allows the optimal calculation of the position and orientation of the forearm (6 degrees of freedom) from 6 sets of coordinates (18 degrees of freedom).

*Comparison of hand trajectories.* A first evaluation of the consequences of parietal inactivation was focused on the analysis of hand trajectories. To this aim we used two approaches, one aimed at assessing significant modifications of the trajectory configuration (shape and dispersion), the other designed to specifically evaluate the change in the spatial dispersion within groups of repeated trajectories under identical movement conditions. The similarity of two hand trajectories were in both instances evaluated by measuring the spatial correlation (R) between the time-series of the velocity vectors of one particular trajectory with those related to a reference trajectory (Shadmehr and Mussa-Ivaldi 1994). For the first analysis, we considered as a reference the means of the control trajectories (MCTs) computed for each arm and for each movement direction and condition (direct and corrected trials), for a total of 24 MCTs. Then, a correlation analysis was made between the individual trajectories observed under different experimental conditions, i.e. before inactivation (Control No-I), under UL-I (left and right), BL-I, and SAL-I and the corresponding MCT. In this way, 160 comparisons for corrected trials (10 reps X 8 conditions X 2 arms) and of

160 comparisons for direct ones (20 reps X 4 movement direction for direct trials X 2 arms) have been performed. This led to 160 R values for each type of movement (direct or corrected) and for each type of experimental condition (Control No-I, BL-I, UL-I left, UL-I right, and SAL-I condition). These Rs were plotted as cumulative distributions (Control No-I: green; UL-I: blu; BL-I: red; SAL-I: yellow) separately for direct and corrected trials. Data obtained from the UL-I of the two hemispheres were pooled together within the same distribution, thanks to the similarities of results when data were considered separately. Finally, for each inactivation condition the relative distribution of Rs was compared, through a Kolmogorov-Smirnov test ( $p < 0.01$ ), with that obtained from the comparisons of the individual control trajectories (Control No-I) with their own means. The second analysis, aimed at evaluating the differences in the dispersion of the hand trajectories within each group of repeated trials, consisted on a procedure in part identical to the one described above, with the only difference that each hand trajectory was compared to its own mean (computed across different replications), instead of the mean of control trajectory (MCT).

*Analysis of eye-hand coupling.* A correlation analysis was performed between the hand and the eye reaction-times during both direct and corrected reaches. This analysis was performed on data obtained before and after muscimol injection. To evaluate the influence of parietal inactivation on the correlation between the two above-mentioned variables, a comparison between pairs of linear regressions was performed to test hypotheses about regression coefficients equality (Zar, 1996) before and after inactivation. For those pairs of linear regressions with slopes not significantly different (ANCOVA,  $p > 0.01$ ), their “common slope” has been computed (Zar, 1996) and then the test for equality of intercepts has been performed.

## RESULTS

### Functional properties of SPL neurons

We will first provide a brief summary of the physiological properties of neurons in the parietal region that was later silenced by muscimol injection. A full account of these properties can be found in Archambault et al, 2009, 2011. The activity of 240 neurons was recorded in the SPL of two left hemispheres of two monkeys while these performed the tasks described above. Microelectrode penetrations (**Fig. 1C**) were made in a region of the SPL identified as Brodmann's area 5 (area PE/PEc). The ANOVA performed (**Fig. 2A**) revealed that the activity of most parietal cells was significantly related ( $p < 0.05$ ) to reaching movements, as it can be inferred by the proportion of them modulated in the different epochs of *Reaching* and *Saccade* task (**Fig. 2**). Furthermore, the majority of cells ( $n=167/240$ ; 70%) were classified as hand-dominant, 20% ( $n=47/240$ ) as eye-dominant, and the remaining ( $n=26/240$ ; 11%) as eye-hand related.

*Hand-dominant cells.* During direct reaches the activity of SPL cells was modulated as a function of the position, velocity and direction of hand movement, as revealed by the regression analysis. During corrected reaches (**Fig. 2B**) the pattern of cell activity associated to the hand movement to the first target changed after presentation of the second one. Cell activity was visibly modulated by hand speed across all the corrected conditions tested. For this cell the multiple-regression yielded an  $R^2 = 0.6$ , and a temporal lag of -70 ms, indicating that the changes in activity led those in motor behaviour.

The multiple regression revealed that all cells displayed a significant relationship between hand kinematics and neural activity ( $p < 10^{-3}$ ). Because of the large number of data points available for the regression analysis ( $n \sim 3500$ ), an  $R^2 = 0.01$  was statistically significant at the 1% level. The distribution of the temporal lags yielding the highest regression coefficient for the population of hand-related cells showed that the activity of most of them had a negative delay, indicating that their modulation led hand movement onset.

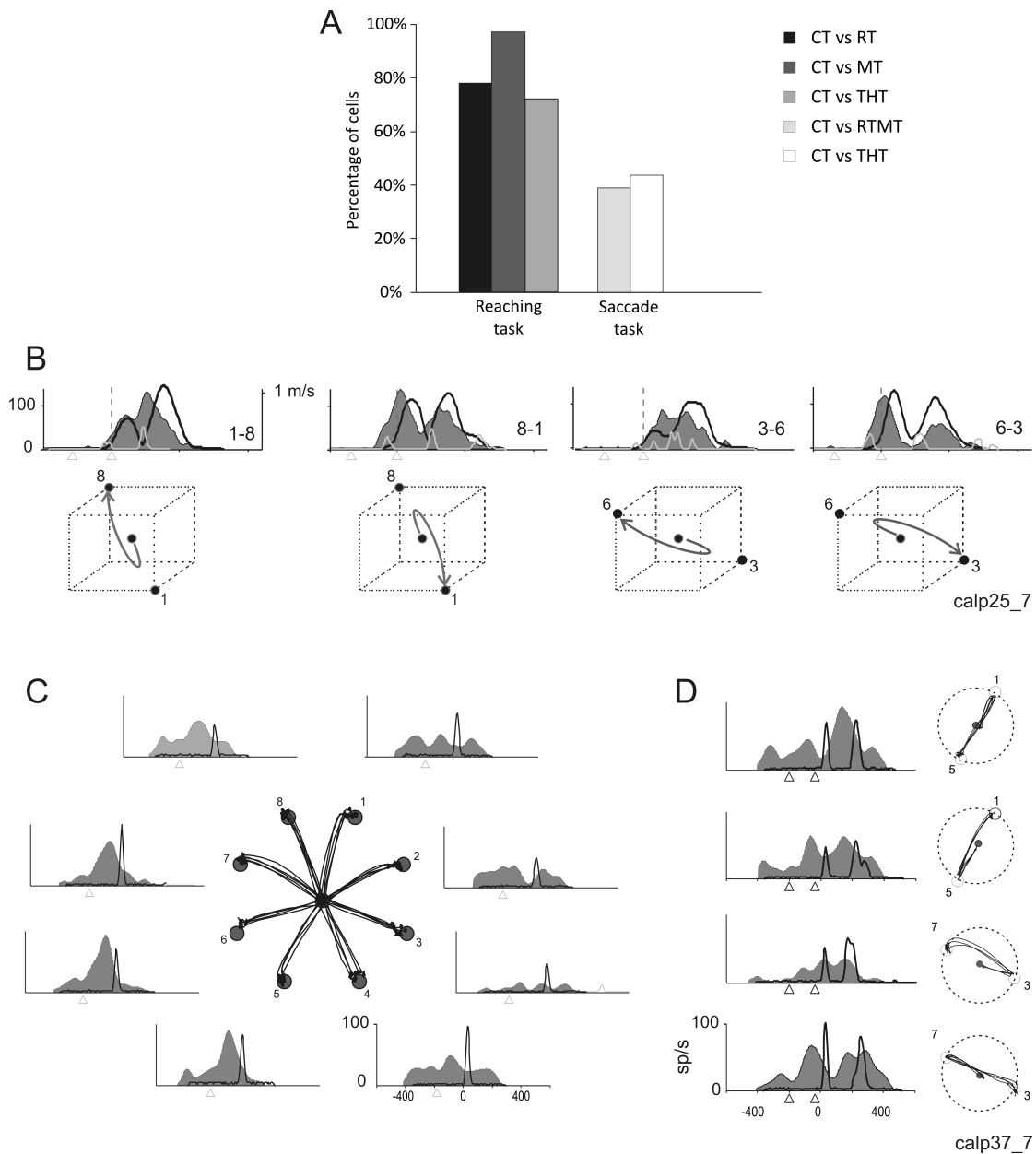


**Figure 2.** Neurophysiological properties of parietal neurons. (A) Proportion of cells significantly modulated during different epochs of the *Reaching* and *Saccade* tasks (ANOVA,  $p < 0.05$ ). Acronyms as in Fig. 1. (B) Neural activity of a parietal cell during on-line corrections of hand movement after target jump at MT onset. Hand trajectories associated to the activities, shown as spike density function (SDF, filled black curve), are displayed in a schematic fashion ( $180^\circ$  target jump). The relative hand (thick grey curves) and eye (thin grey curves) speed profiles collected during neural recording are superimposed. The triangles indicate the mean time of first and second target presentation; 0 ms corresponds to of hand movement onset. (C-D) Neural activity of a parietal cell studied during *Single-* (C) and *Double-step* saccades (D), with relative eye trajectories. Temporal alignment (0 ms) corresponds to eye movement onset. Conventions and symbols as in (B).

*Eye-dominant cells.* During direct saccades to visual targets (**Fig. 2C**) the modulation of cell activity mostly led the onset of the saccade. When a second target was presented during eye-RT (**Fig. 2D**), the eye completed the saccade to the first target and then moved to the second one. In such instances, cell activity could be predicted by the activity pattern associated to the two direct eye-movements performed in sequence, as shown for hand related-cells (Archambault et al., 2009).

### **Behavioral data**

*Hand reaching movement.* During direct reaches (**Fig. 3A**), the hand moved directly to the target with a slightly curved trajectory that was similar for all movement directions. During corrected reaches (**Fig. 3A**), the hand initially moved towards the first target and then suddenly curved toward the second one. In absence of corrections the hand described a typical bell-shaped velocity profile (**Fig. 3B**), while, when a correction of trajectory was required, the hand velocity profile displayed two peaks (**Fig. 3B**). The first one was characterized by an initial acceleration, followed by a deceleration at the end of which the change of direction of the hand movement toward the second target occurred; then, a second acceleration occurred, at the end of which the hand attained the highest peak in speed, to decelerate again and land on the target. The overall shape of the hand velocity profile also depended on the time of occurrence of target change. When the second target was presented at the onset of hand movement, the deceleration following the first velocity peak was longer than the corresponding one observed when the target jumped during the reaction-time.

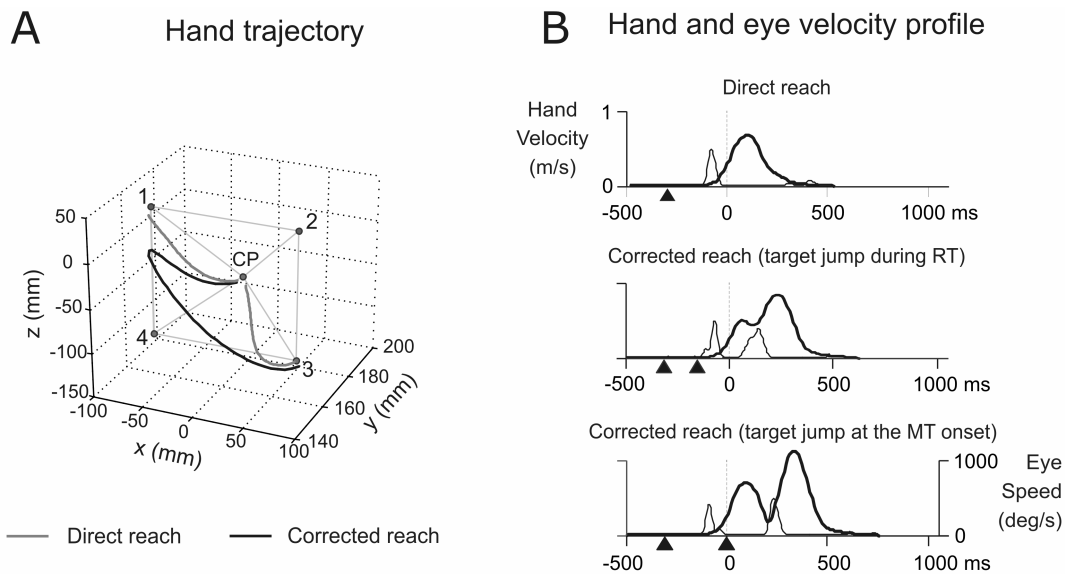


**Figure 3. Behavioral data under control condition.** (A) Examples of real hand trajectories in two direct (grey) and in one corrected reach (black). CP denotes the position of the central target, numbers indicates the four peripheral targets used in the inactivation experiment. In the example of the corrected reach, the hand moves first toward the target 1 (as for the upper direct reach) and then makes a 180° correction toward the target 3 (similarly to the lower direct reach). (B) Hand (thick curve) and eye (thin curve) velocity profile during direct reaches and during corrected ones with target jump occurring at two different times. Conventions and symbols as in Fig. 2.

*Consequences of muscimol injection on hand reaching.* We first analysed the effects of parietal inactivation on hand trajectories, by comparing their shapes and dispersion to the controls recorded in absence of any injection (**Fig. 4A**) and after saline injection. After BL-I hand movement trajectories in many instances were more variable and dispersed in space than control ones (**Fig. 4A**). In fact, the comparison of individual trajectories collected during control condition and after UL-I and SAL-I with their respective MCT (see Methods for details) yielded in the majority of cases a correlation close to 1. On the contrary, the distributions of the R coefficients (**Fig. 4B**) showed that bilateral inactivation (red distribution) led to significant decrease of R's values (K-S test,  $p < 0.001$ ) relative to those obtained from the control condition, as well as from UL-I and SAL-I. This decrease was observed for both direct and corrected reaches (**Fig. 4B**). Since smaller Rs values can either indicate that the hand trajectories had different shapes or that they were more dispersed in space as compared to control ones, the contribution of the spatial dispersion was assessed



through a second analysis. This was performed by comparing for each experimental condition every single hand trajectory to the mean one computed across the 10 replications of each movement condition. The results showed that in this case there was no significant difference between the distribution of Rs obtained before and after BL-I. Overall these results suggest that the shape rather than the spatial dispersion of hand trajectory was affected by the bilateral SPL inactivation.

From now on in the manuscript, we will only illustrate the effects of BL-I, the only one that had significant consequences on the behaviour of both animals. **Figure 5A** illustrates the effect on the RTs (toward the first target) of the right and left arm for both monkeys.

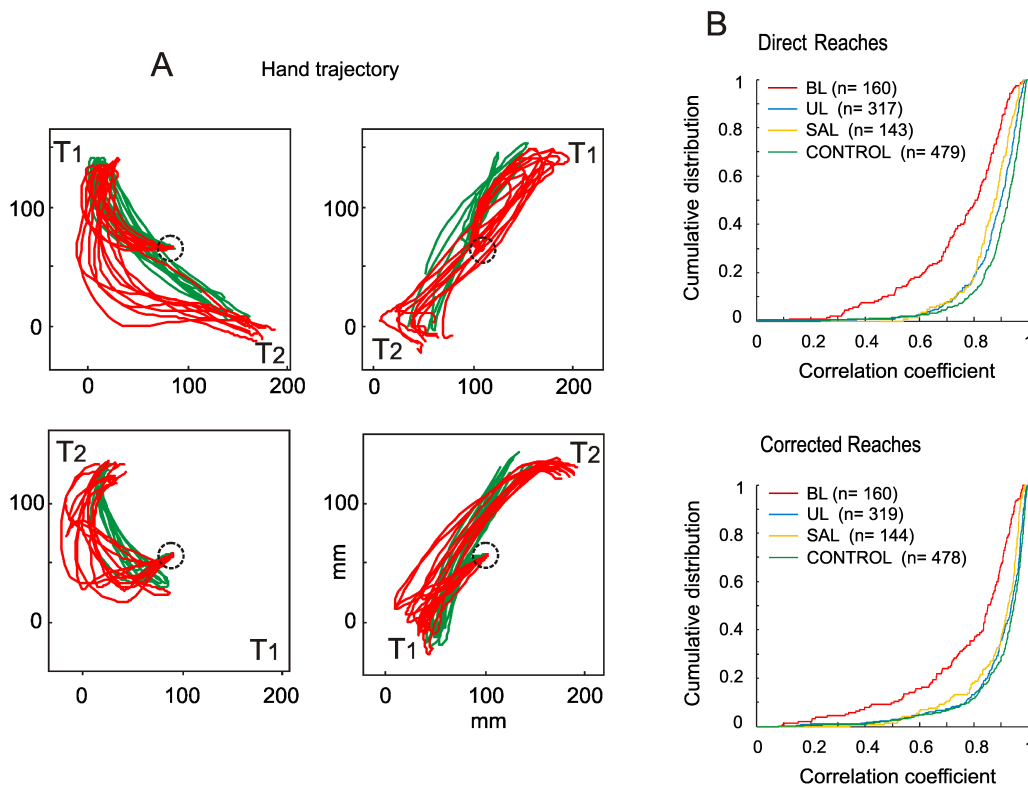


**Figure 4. Effects of parietal inactivation on hand trajectories.** (A) Repeated hand trajectories in 4 different types of movements, before (green) and after BL-I (red). (B) Quantitative assessment of the change in the trajectory features under different conditions (*direct* reaches and *corrected* reaches). Plot of the cumulative distributions of the correlation coefficients obtained from the comparison of the individual hand trajectories observed under BL-I (red), UL-I (blue), SAL-I (yellow) and before injection (green) to the relative mean control trajectory (MCT), taken as a reference. The distribution referring to BL-I (red) is significantly different for both *direct* (K-S test,  $p < 0.001$ ) and *corrected* (K-S test,  $p < 0.001$ ) reaches from that relative to control trajectories (green), and from those obtained after UL-I or SAL-I, that showed little or no effects relative to controls. Data are from Monkey 1. Similar results were obtained in Monkey 2.

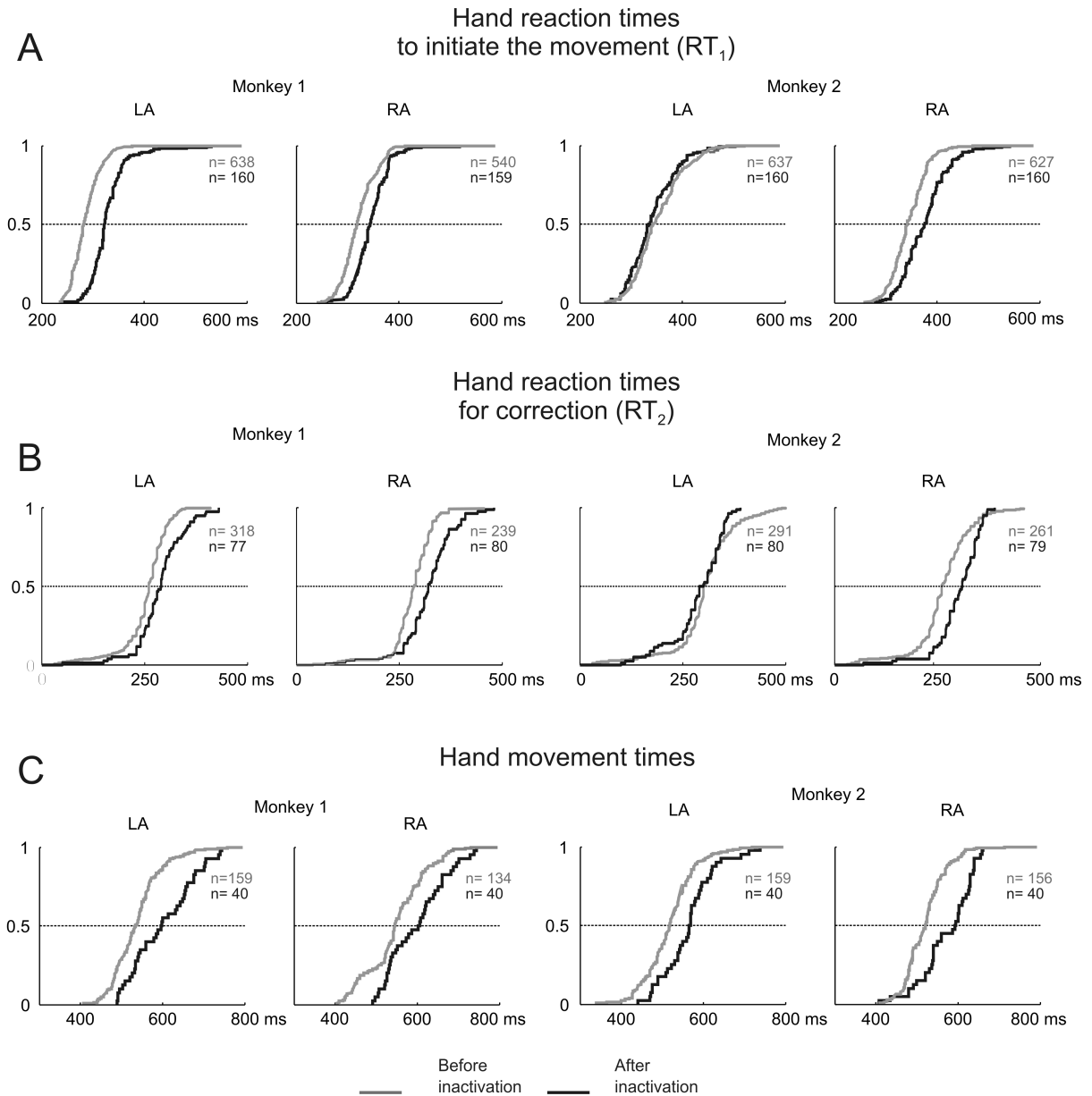


**Figure 5.** Effects of parietal inactivation on the timing of hand behaviour. Cumulative frequencies distributions comparing the hand reaction-time (RT) to the first target (A), hand RT to the second target (B) and movement-time (MT, C) before and after BL-I. In A, RT is relative to the appearance of the first target (data pooling from *direct* and all types of *corrected* reaches). In B, RT is measured from the appearance of the second target to the switch time of hand trajectory in the *corrected* reaches. MT data refer to *corrected* trials, when the target jumps at the MT onset. In all graphs the control times (grey line) were obtained from pooling the data of control tests of four different sessions. Experimental data (black line) were obtained from a single injection session (BL-I). Numbers on each panel refer to amount of trials for each condition. LA and RA indicates left and right arm, respectively.

Since for this variable no differences has been observed across reaching conditions, the data from direct and corrected trials were pooled together. In all cases, but left arm in Monkey 2, a significant increase (K-S test;  $p < 0.001$ ) of the hand RT to the first target (mean increase of  $RT_1$  : 42.8 ms in Monkey 1, 31.5 ms in Monkey 2) was observed. In both monkeys (for movement performed with either left or right arm) a significant increase of the time elapsing from the presentation of the second target to the time of reversal of hand trajectory ( $RT_2$ ) was also observed (mean increase of  $RT_2$  : 45 ms in Monkey 1, 30 ms in Monkey 2). Concerning the duration of MT, a significant elongation (K-S test;  $p < 0.001$ ) was observed in both monkeys during corrected reaches for both right and left arms (**Fig. 5C**), when the target jumped at the onset of hand movement. In the other movement conditions (direct and corrected reaches with target jump during RT) an increase of MT after BL-I was observed only in one monkey. On average the difference between the mean MT before and after inactivation was of 58.0 ms in Monkey 1 and of 50.0 ms in Monkey 2. A clear picture of the effects on timing of hand movement can also be seen in a movie (Supplementary Material) created from the time-sequence of the instantaneous positions of the hand during the entire duration of the trial. Hand RT and MT were not affected by saline injection.

When a change of target location occurred (**Fig. 6A**), the hand path toward the first target was longer after BL-I, as compared to control. As a consequence, in-flight trajectory correction was delayed, as also shown by the observation that the double-peaked velocity profile typical of corrected reaches was shifted in time by about 130 ms (**Fig. 6B**).

To better understand the nature of this delayed correction of hand trajectory, a linear regression between the hand velocity curves of control trials vs. those obtained after muscimol injection was performed. First, the corresponding curves were aligned to the onset of hand movement to the first target (**Fig. 6C**). The time-lag of 40 ms was obtained between the correlated ( $R=0.989$ ) rising phases of the hand velocity profiles toward the second target, suggesting that a delay occurred in the adjustment of the hand trajectory after muscimol injection. When the velocity profiles were aligned to the onset of hand movement

to the second target (**Fig. 6D**), a second time lag of 90 ms was detected under BL-I relative to controls ( $R=0.999$ ), indicating a delayed execution of hand movement toward the second target.

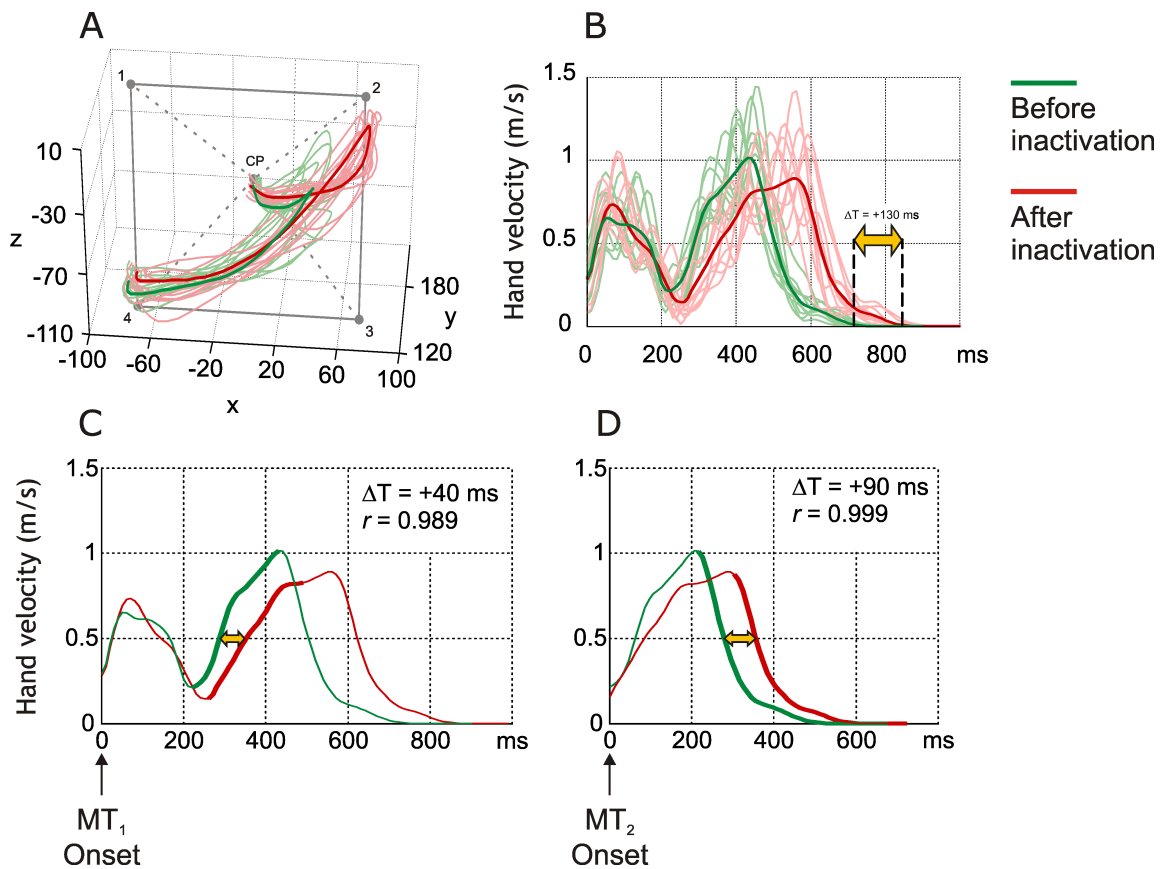


**figure 6.** Effects of parietal inactivation on the length of hand-path and hand speed. (A) Replications of individual hand trajectories (thin curves), and their mean (thick curve) from a central position (CP) during corrected reaches with the right arm, after target displacement at the onset of hand movement (from target 2 to target 4) before (green) and after BL-I (red). (B) Hand speed profiles relative to the movements shown in (A). Notice the shift (+ 130 ms) of the double-peaked speed profile typical of corrected reaches after BL-I. To highlight the nature of the effects of parietal inactivation on hand speed, the mean velocity profiles shown in B have been plot by adopting two different alignments: at the onset of hand movement ( $MT_1$ ) toward the first target (C), and at the onset of hand shift toward the second target ( $MT_2$ ), i.e. at the time when the hand speed reaches its minimum to reverse the movement in the opposite direction (D). The thicker part of the curves are those on which a regression analysis was performed (corresponding time-lag and correlation coefficient are shown).

*Eye movements.* Eye movements were monitored during direct saccades (*single-step*) and in *double-step* trials. Under control conditions, during single-step saccades the eye moved toward the visual target (**Fig. 2C**), with mean peak velocity of 751 ( $\pm$  219 SD) deg/s in Monkey 1 and 644 ( $\pm$  36 SD) deg/s in Monkey 2. When a second target was presented during RT, the eye completed the saccade to the first target and then moved to the second one (**Fig. 2D**). During double-step trials, eye movements were characterized by a double-peaked velocity profile (**Fig. 2D**), with the peak velocity to the first target similar to that seen during single-step saccade. The mean peak velocity to the second target was 1055 ( $\pm$  181) deg/s in Monkey 1 and 890 ( $\pm$  113) deg/s in Monkey 2, and it was significantly higher (t-test,  $p < 0.001$ ) than that to the first target. The eye  $RT_1$  was 148 ( $\pm$  25) ms in Monkey 1 and 123 ( $\pm$  16) ms in Monkey 2, while  $RT_2$  was  $178 \pm 15$  ms in Monkey 1 and  $138 \pm 14$  ms in Monkey 2. Thus, the eye RT to the second target was significantly (t-test,  $p < 0.001$ ) longer than that to the first one. See also the example shown in the movie (Supplementary Material) of the reconstruction of eye movements in the space and time domains.

*Consequences of muscimol injection on eye movement.* After BL-I the endpoints of eye movements in the single- (**Fig. 7A**) and double-step trials (**Fig. 7B**) were similar to those of controls, as it can be seen from the analysis of their dispersion around the mean. The similarity of the saccade end-points across conditions was assessed measuring the deviations of each endpoint from the mean position in a given location, along the  $x$  ( $Dx$ ) and  $y$  ( $Dy$ ) axis (**Fig. 7C**), and by comparing their relative distributions (K-S test,  $p < 0.01$ ). It can be noticed that the second saccades of the *double-step task*, as compared to those of the *single-step task*, were more dispersed, although in a similar fashion, before and after parietal inactivation. The different amplitude of the second saccade, which was twice longer than the first, can explain this phenomenon, since the endpoint accuracy of saccades decreases with their amplitude (van Opstal and van Gisbergen 1989; van Beers 2007). In both monkeys, the eye velocity profiles to the first and second target were not affected by BL-I.

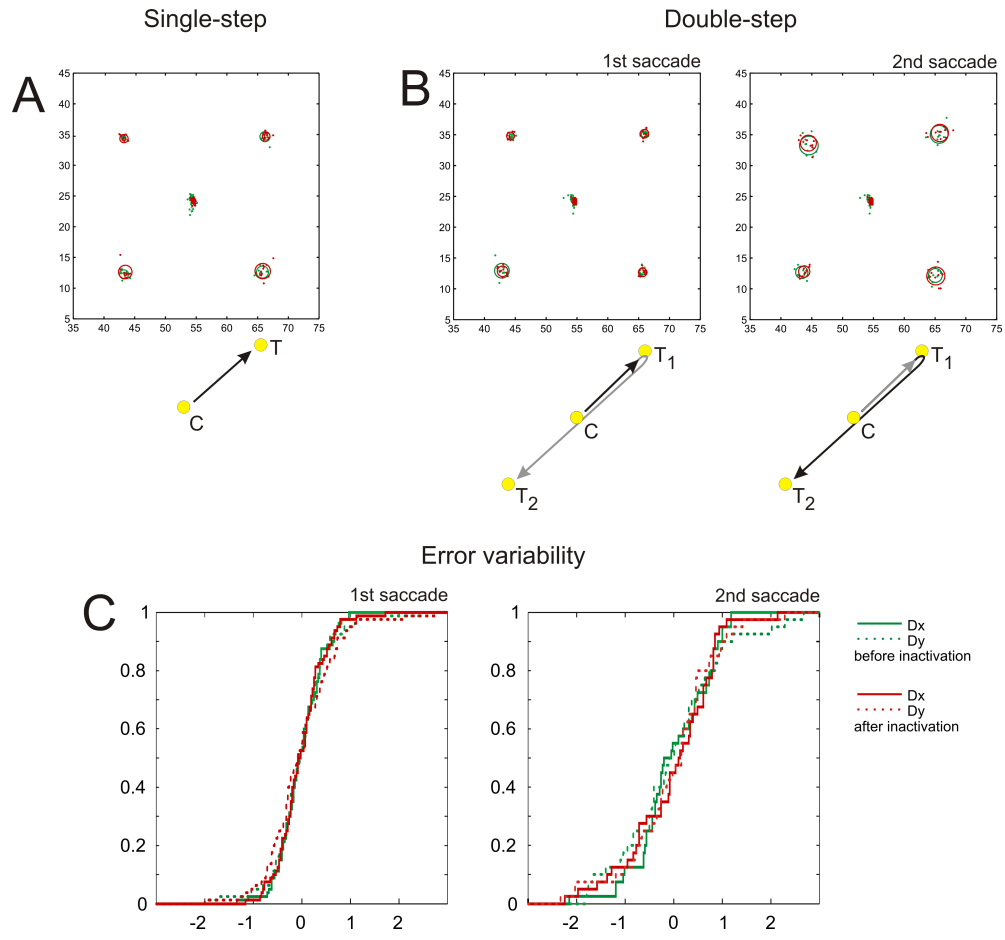


**Figure 7.** Endpoints of saccades in the Single-step (A) and Double-step (B) saccade tasks, before (green) and after (red) BL-I. In A the saccades start from the central target (C) and achieve the peripheral one (T). (B) *Left*, the endpoints refer to the first saccade (from C to the first target, T<sub>1</sub>). *Right*, endpoints refer to the second saccades (from T<sub>1</sub> to T<sub>2</sub>). Note the different amplitude of the first and second saccades in the Double-step condition. In each location, the empty circle represents the dispersion around the mean position of the endpoints, being its radius equal to the mean of SD<sub>x</sub> and SD<sub>y</sub> (corresponding to the SD of errors along x and y axis, respectively). (C) Cumulative distributions of deviations from the mean along the x (D<sub>x</sub>, solid line) and y axis (D<sub>y</sub>, dashed line), before (green) and after inactivation (red). The distributions refer to endpoints of the first saccades (Single-step and Double-step task) and second saccades (Double-step task), separately.

The main effect was observed on saccade timing (**Fig. 8**). The mean eye RT<sub>1</sub> was 175 (± 20) ms in Monkey 1, and 135.7 (± 11.8) ms in Monkey 2, while mean RT<sub>2</sub> was 246 (± 12) ms in Monkey 1 and 158 (± 10) ms in Monkey 2 (**Fig. 8A**). Thus, the saccades to the first and second target were both significantly (t-test, p<0.001) delayed relative to control trials. The elongation of RTs, particularly of RT<sub>2</sub>, is also evident from the eye speed profiles of 20 collected trials (**Fig. 8B**), when the eye moved in four different directions.

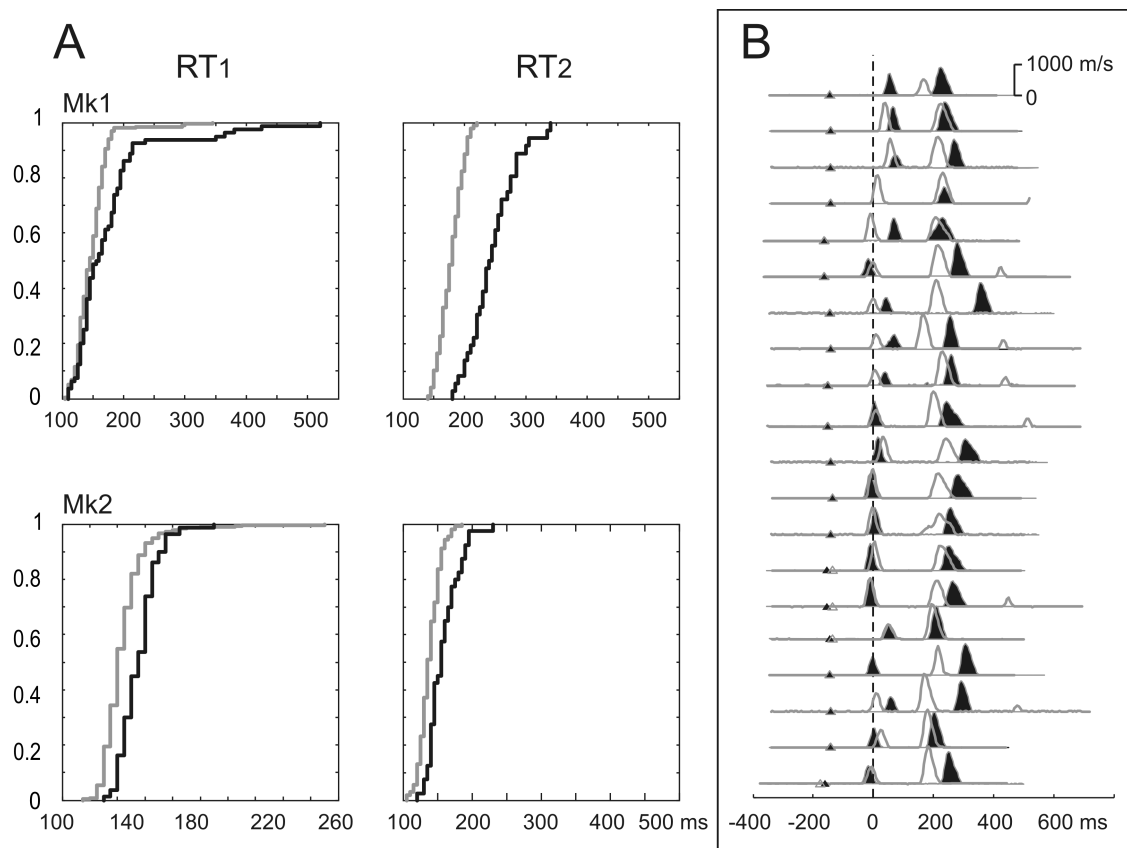


**Figure 8. Effects of muscimol on timing of saccadic eye movements in the Double-step saccade task.** (A) Cumulative frequency distributions of RT<sub>1</sub> and RT<sub>2</sub>, under control conditions (grey) and after BL-I (black), in both monkeys (Mk1 , Mk2). In all cases, the difference between the two conditions was significant (K-S test, p<0.001). (B) Replicas (n. 20) of eye velocity profiles under control condition (grey) and after BL-I (filled black) in Mk1. Grey and black triangles indicate the time of the first target presentation under control condition and BL-I, respectively; 0 ms (vertical interrupted line) indicates the time of second target presentation.

*Consequences of muscimol injection on eye-hand coupling.* We studied whether the delays observed in the reach tasks were consequence of the above described eye impairment. For this purpose, the correlation between the hand and the eye RTs to the first (RT<sub>1</sub>; **Fig. 9A**) and second (RT<sub>2</sub>; **Fig. 9B**) target was studied before and after BL-I for the datasets in which parietal inactivation led to a significant increase of the hand RT<sub>1</sub> and RT<sub>2</sub> (**Fig. 5A-B**).

It is worth remembering that the hand RT<sub>2</sub> corresponds to the time of hand switch, therefore it was studied in relation of the saccade RT to the second target. The correlation between hand and eye RTs was analysed for four different datasets (2 monkeys, both tested with left and right arm) and was found to be significant in all of them before, as well as after BL-I ( $r$  ranging from 0.3 to 0.5), the only exception being the control data in Monkey 1 (right arm), in which hand RT<sub>2</sub> was not significantly correlated with the eye RTs to the second target ( $r= 0.22$ ,  $p=0.06$ ). We then focused on those cases for which an increase of hand RT<sub>1</sub> and RT<sub>2</sub> was obtained after BL-I, to test whether this impairment depended from the oculomotor deficit and, if so, to which extent.

It has been found that the hand and the eye RT<sub>1</sub> (**Fig. 9A**) were similarly correlated before and after BL-I, as evidenced by the lack of a significant difference between the slopes of the two linear regressions, that were therefore plotted with their common slope (see Methods). This implies that the increase of the hand RT<sub>1</sub> after injection can be, at least in part, explained by the observed increase of the eye RT<sub>1</sub>. However, parietal inactivation yielded to a further increase of the hand RT<sub>1</sub>, which cannot be accounted by the elongation of eye RT<sub>1</sub>, as concluded from the significantly higher value ( $p<0.001$ ) of the intercept of the linear regression for the data obtained under this condition. In the corrected reaches, the pre-existing significant correlation ( $p<0.001$ ) between the hand RT<sub>2</sub> and the eye RT<sub>2</sub> (**Fig. 9B**), observed during control testing, remained similar following BL-I (as in the case of RT<sub>1</sub>, the common slope of the two regressions has been plotted). However, contrary to what has been observed to RT<sub>1</sub>, a negligible or no increase of intercept has been observed. For the dataset relative to Monkey 1 (right arm) where in normal condition the regression was not significant, BL-I led to the emergence of a significant correlation between hand and eye Rts.



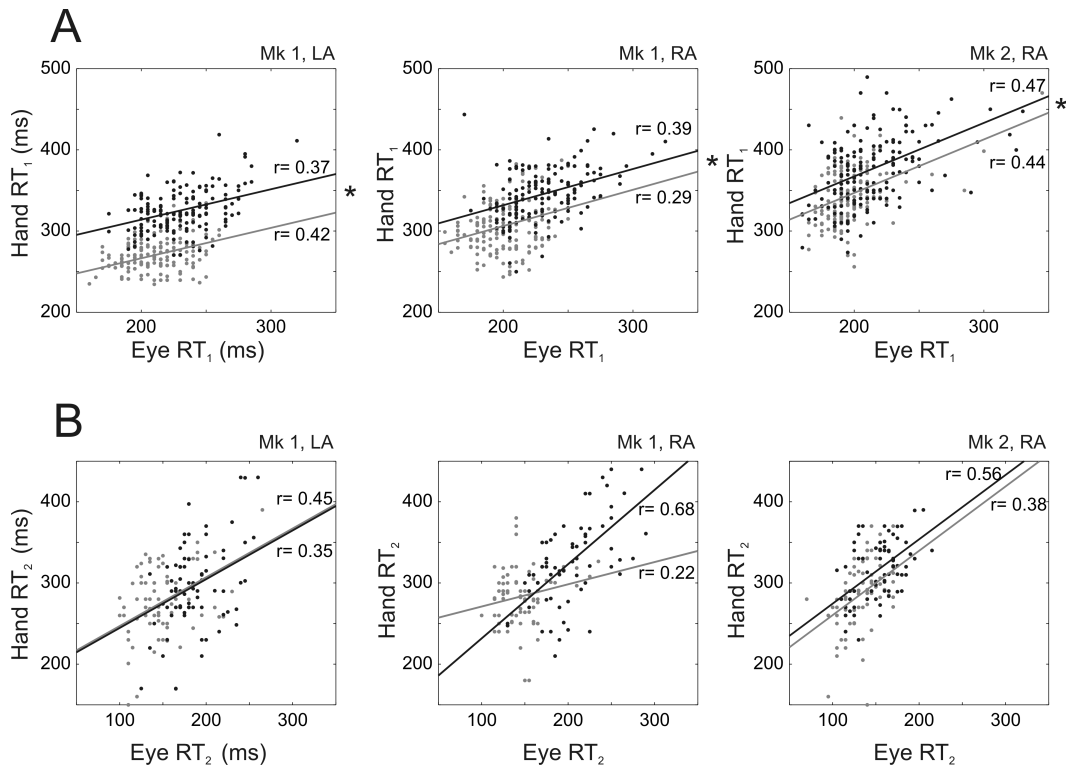


**Figure 9. Correlation between eye and arm reaction times**, before (grey) and after parietal inactivation (black). (A) Eye and hand RTs refer to those recorded during *direct reaches* and to those relative to movements toward the *first* target during *corrected reaches*. (B) Correlation between eye RT<sub>2</sub> (time elapsing from the appearance of the second target and the onset of the second saccade toward it) and hand RT<sub>2</sub> (time elapsing from the appearance of the second target and the change in direction of hand trajectory), collected during *corrected reaches*. In A and B eye-hand correlation has been restricted to datasets (Monkey 1, left and right arm; Monkey 2, right arm) that showed a significant increase of hand RTs (see Fig. 5A-B). Correlation coefficient ( $r$ ) is reported for each linear regression. Asterisk (\*) indicates highly significant differences ( $p < 0.001$ ) between intercepts of two linear regressions (grey and black lines). For details about linear regression see Methods.

Overall the results shown in **Fig. 9B** suggest that the elongation of the time necessary to update hand movement direction can be largely explained by the delayed eye movement to the second target. It is worthwhile noticing that for both  $RT_1$  and  $RT_2$ , BL-I led to an increase of the dependence of the hand from the eye behaviour, as it can be inferred by the higher  $r$  values measured after inactivation, particularly when looking at the times needed to update hand movement toward a new direction ( $RT_2$ ).

## DISCUSSION

### *On-line control in fast reaching*

The inactivation of the SPL affected both the timing and the kinematics of hand reaches. In both the direct and corrected trials we observed a significant elongation of the hand reaction-time to the first target; similarly, an increase of the hand reaction-time to the second target was detected in the corrected trials. When the target jumped at the onset of hand movement, corrective reaches were slower than controls. In control conditions, after target jump the hand smoothly changed trajectory to land on the new target location. After muscimol injection, the hand path toward the first target was significantly longer, due to a delayed trajectory correction.

An in-depth analysis of the hand velocity profile revealed that a first delay occurred at the moment of the trajectory update, consisting in the lengthening of the reaction-time to the second target. A second delay was observed during movement-time toward the second target. Thus, both the preparation and execution of the corrective reach were delayed in time by SPL silencing.

An additional deficit consisted in a change in shape, rather than on spatial dispersion, of the hand movement trajectories relative to controls. This reveals an impaired selection of the shorter and most appropriate hand path (Morasso, 1981) to the target, or it can be consequence of the disturbance of the mechanism which seems to be common to the formation of both unperturbed and corrected reaching movements (d'Avella et al. 2011), for which the SPL can be regarded as a central neural node. However, the constant pattern of trajectory curvature observed after SPL inactivation raises the possibility that the impaired performance can be consequence of the breakdown in the transformation of the desired hand path into a sequence of appropriate joint rotations and/or in the control of the posture and geometry of the arm during hand reach (Lacquaniti et al. 1995).

These results provide the first available model of Optic Ataxia in monkeys, at least as far as one of its main features is concerned, i.e. the impaired on-line control of hand movement. In humans bilateral parieto-

occipital lesion results in delayed on-line correction of hand trajectory and elongation of hand path toward the second target (Pisella et al. 2000; Grea et al. 2002), a clinical picture fully reproduced by our result, which also conform to the conclusion of studies of perturbation of parietal cortex through TMS (Desmurget et al. 1999; Johnson and Haggard 2005). Furthermore, our results indicate that the SPL is a crucial node for on-line control of hand movement trajectory, an argument on which the above mentioned studies in humans could not be conclusive, either for the size of the natural lesion or for the uncertainty on the extent of the parietal region perturbed by TMS stimulation. Our results also conform to those of a fMRI study of the brain areas activated by different types of reach errors (Diedrichsen et al. 2005), that attributes to the posterior SPL a specific role in online corrections after target displacement.

We did not detect constant and significant effects after unilateral inactivation of SPL. The need of a bilateral inactivation of parietal cortex to impair on-line visual control of hand movement, which normally occurs in central vision, might be dependent on the concurrent processing of both hemispheres under this condition. However, it cannot be excluded that muscimol injections involving a larger SPL region could result in deficits of on-line control. Ongoing research in humans in our lab and the results of a large study group of parietal patients (T. Shallice, personal communication) indicate that unilateral SPL lesion in humans results in deficit of on-line control of hand movement.

#### *Saccade control*

Together with reaching deficits, our study shows for the first time that the bilateral inactivation of the SPL resulted in defective timing of saccades. After target jump, the eye did not interrupt the saccade to the first target, as the hand did, but made two consecutive saccades, originally toward the first target's location, then to the second one. These movements had normal peak-velocity and spatial dispersion of their endpoints, in both single and double-step trials. However, a delayed onset of the saccade to both the first and the second target was observed, suggesting that, as for the hand, the parietal inactivation impaired the timing of the composition of both the original and new motor command. This result is consistent with the

presence of populations of pre-saccadic cells whose signals are combined with hand-related information in this segment of the parieto-frontal network (Battaglia-Mayer et al. 2000; 2001; see Caminiti et al. 2010, for a review).

#### *The role of parietal cortex in the control of coordinated hand-eye movement*

Studies where healthy subjects “look and point” to visual targets have highlighted a clear temporal coupling between eye and hand movement. A tight correlation between the time of initiation of eye movement (eye RT) and that of hand (hand RT) has been found when looking and reaching toward a common visual target (Herman et al, 1981). Varying degree of correlations ranging from moderate (Prablanc et al. 1979) to high (Gielen et al, 1984; Neggers and Bekkering 2002) have been reported during reaches with target displacement. The correlation reported by these studies during corrected reaches is significantly different from that observed during direct ones, if the target jumps during RT, and the interval between the first and the second target presentation is greater than 125 ms (Gielen et al, 1984).

Despite the large evidence of a functional link between eye and hand movement, not only in humans but also in monkeys (Snyder et al, 2002), neuropsychological studies of Optic Ataxia have basically ignored the analysis of the eye movement which naturally leads hand reaching, mostly because patients are usually requested to keep fixation constant while reaching at peripheral targets, a condition believed as necessary to reveal Optic Ataxia. Since the impairment in eye movements often consists in a short increase in latency of saccade initiation, this cannot be detected without a quantitative control of oculomotor behavior. Furthermore, when impaired eye movements were observed, they have been considered irrelevant for the hand misreaching (Baylis and Baylis, 2011, Perenin and Vighetto 1988). This conviction has been strengthened by the belief of the existence of a parietal “saccade” system, strictly segregated from that dedicated to hand movement, both in humans (Pierrot-Desilligny et al. 2004) and monkeys (Andersen et al. 1992), and by the observations that after parietal lesion impairments of eye and hand movement can occur in isolation. However, several neurophysiological studies on humans and monkeys have pointed to the

existence of a functional link between eye and hand movement (Battaglia-Mayer et al. 2000; for a review see Caminiti et al. 2010) in most cortical areas belonging to PPC, as also shown by the observation that the degree of effector selectivity during reaches and saccades is rather low in different areas of parietal cortex, not only in monkeys, but also in humans (Levy et al. 2007; for a review see Filimon, 2010).

A recent study (Gaveau et al, 2008) was aimed at investigating ocular control in Optic Ataxia, testing two patients with bilateral parietal lesion in a natural “look and point” paradigm with target jump. Both subjects exhibited a delayed visual capture, showing an impairment of fast saccade control. This resulted in a modification of the temporal sequence of eye-hand coordination, consisting in a delayed pointing to visual targets. In particular, patient AT showed a marked increase of about 200 ms in eye RTs, followed by a larger increase of hand RT larger than 400 ms. Our observations are in agreement with these results. In fact, it is worth noting that the reported delayed initiation of hand movement in parietal patients can be, at least in part, explained by the elongated eye RTs. However, its value (about two times higher relative to eye RT, as reported by Gaveau et al. 2008) points to the existence of a further independent impairment in the hand movement initiations after parietal lesions, as similarly suggested by the significant increase, after parietal inactivation, of the intercepts of the linear regressions that link eye and hand RTs (Fig. 9A). During corrections, our results showed that the elongation of the time necessary to reverse hand movement direction is instead largely influenced by the delayed oculomotor behaviour.

Overall, the behavioral defects observed after reversible inactivation of the SPL seem to be dependent both on the impaired timing of composition of a new motor command, which is reflected in the delayed planning and, as far as the hand is concerned, on an altered shape and length of the hand trajectory, probably resulting from both planning and execution errors. The planning phase of reaching movement is however undoubtedly influenced by the associated saccade occurring before the hand movement. Therefore the impaired fast ocular control, consisting in the elongation of the saccade to the visual target, might be regarded as a potential source of the delayed manual correction after parietal lesions, to be added to a parallel impairment in the control of the hand trajectory. This is not surprising, since both eye and hand

reach defects can be expected when considering the functional properties and the cortico-cortical connectivity of the SPL areas silenced by muscimol injection. Areas PE mostly encodes somato-motor information about limb position and movement direction (Lacquaniti et al. 1995; Archambault et al. 2009) and projects directly to motor cortex (Johnson et al. 1996), while its most caudal part (area PEc), in addition to somatosensory information also receives significant visual and eye-related inputs (Battaglia-Mayer et al. 2001; Squatrito et al. 2001; Marconi et al. 2001; Bakola et al. 2010) and projects to dorso-caudal premotor cortex (PMd/F2; Marconi et al. 2001; Bakola et al. 2010), which in turn projects to motor cortex. In PEc neural activity is also related, among other functions, to planning of eye-hand movement (Battaglia-Mayer et al. 2001). Therefore in the functional gradient of the SPL all information about target localization, eye and hand position, movement direction and speed, as well as preparatory signals coexist and, as previously shown, are combined in a coherent fashion in the *global tuning field* (Battaglia-Mayer et al. 2000, 2001) of individual neurons. This information is crucial for the utilization of target location signals necessary for reach planning and its continuous update. The collapse of this combinatorial mechanism may results in a cascade of behavioral defects, such as those observed in monkeys after reversible inactivation of these parietal areas, thus providing a “positive image” of Optic Ataxia in man (Battaglia-Mayer and Caminiti 2002; Caminiti et al. 2010).

## SECTION 2

**Optic ataxia generalizes to hand movement under isometric conditions**



## INTRODUCTION

Modern views on sensorimotor transformation underlying reaching to visual targets hold that reach plans are represented simultaneously in different reference frames to allow optimal remapping and task-dependent reweighting of available sensory signals (Battaglia-Mayer et al., 2003; McGuire and Sabes, 2009; Caminiti et al., 2010). Under this assumption, lesions of the cortical areas involved in such transformation, such as posterior parietal cortex (PPC), should result in similar reach defects regardless of the type of signals to be aligned and, and therefore of the remapping required.

We asked a patient with acute Optic Ataxia (OA) from unilateral tumor lesion of the right superior parietal lobule (SPL) and of the intraparietal sulcus (IPS) and a group of normal age-matched control subjects to perform conventional reaching movements from a central position, aligned to the body midline, to peripheral visual targets presented on a touch-screen, and to perform a similar center-out task under isometric conditions, where no hand movement had to be made, but only a force had to be applied to an isometric joystick to move a visual cursor to peripheral visual targets. Both tasks were performed under two conditions, in the first the eyes were allowed to move toward the visual targets (foveal condition), in the second subjects were requested to maintain central fixation while reaching to eccentric targets (extrafoveal condition).

We wanted to assess whether Optic Ataxia emerges not only when a movement requiring the arm and hand displacement is performed, but also where only a force pulse of desired strength and direction is generated. In the former case, during movement planning the brain needs to align visual information about target location and proprioceptive signals about hand position to generate a hand displacement vector of appropriate direction and amplitude to bring the hand to the target. In isometric conditions such computation first requires remapping the position of the hand into that of the visual cursor, as to account for the dissociation between the visual display, where targets are presented and the visual cursor is moved, and the manipulandum on which forces of different directions are applied. Furthermore, in the isometric

condition remapping concerns visual signals from the moving cursor on information from the hand/arm force receptors. In other words, during natural reaching vision and kinesthetic information have to be combined, in the isometric condition vision and force signals.

We found that the patient showed reach defects, mostly to eccentric targets, regardless of whether movement was performed in isometric conditions or consisted of a physical displacement of the hand, thus generalizing to isometric conditions the reach defects observed for conventional reaching movements.

## METHODS

### Subjects

Patient F.D.L. is a right handed 19 years old male who went to observation for a mild, although persistent, somatosensory deficit to the left hand. The MRI scan revealed a large unilateral lesion that on the histological exams resulted to be a high grade glioma (**Fig. 1**) centered on the right superior parietal lobule (SPL, Brodmann's area 2, 5, and 7), affecting both banks of the IPS, and extending to the precuneus (Brodmann areas 7 and 31) on medial surface, anteriorly to the parieto-occipital fissure. The cortical involvement was defined according to volumetric T1 Inversion Recovery sequence analysis on 3 T MRI scanner (Verio, Siemens AG, Erlangen, Germany). On the white matter, the pathological process involved the dorsomedial superior longitudinal fasciculus (SLF) just posterior to the superior aspect of the corona radiata, according to Wakana et al (2003). The white matter involvement of the SPL and precuneus included subcortical, subgyral, gyral and lobar sectors, according to Yasargil et al. (1994). Long association fibers involvement was studied with 32-directions fiber tract analysis at 3.0 T MRI.

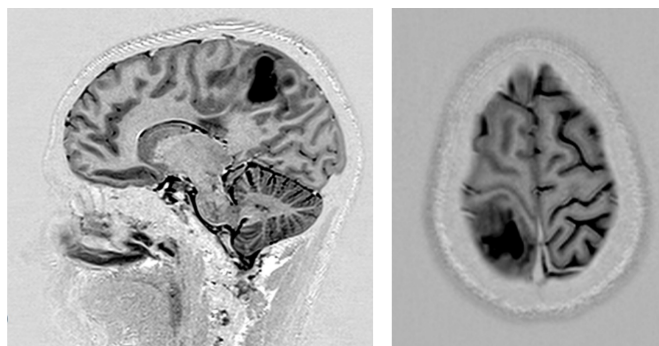


**Figure 1 – MRI scan of patient's lesion site.** Patient FDL shows a large unilateral lesion centered on the right superior parietal lobule, affecting the SPL and both banks of the IPS, and extending to the precuneus on medial surface, anteriorly to the parieto-occipital fissure.

Beyond the reduction of tactile sensation on the left hand, standard clinical tests did not reveal any primary sensory or motor impairment. Muscle tone, reflex activity and joint sensation and motion were all as in normal controls. A set of standard neuropsychological tests revealed a manifest Optic Ataxia, consisting of large reach errors with the left hand to targets presented both in the left (contralesional) and right visual fields, and with the right hand mainly in the left visual field. These deficits were evident for reaches in both central and peripheral vision, but were larger when reaching was made to extrafoveal targets.

Eight age-matched control subjects were also studied. All subjects had normal or corrected-to-normal vision and gave informed consent to participate in the experiment. Experimental procedures on FDL and controls were approved by the ethical committee of the University of Rome SAPIENZA.

### **Apparatus and tasks**

Patient F.D.L. and the controls were asked to perform hand movements under two different conditions, the *Reaching task* and the *Isometric reaching task*.

#### *Reaching task*

All the subjects performed the task while seated in front of a 21 inches touch-sensitive (MicroTouch Systems, Wilmington) computer monitor used to display the task and to control the hand position (**Fig. 2A**). Arm movements originated from a central push-button located 20 cm from the screen and aligned to the body midline and were directed toward six peripheral targets (subtending 10° of visual angle) located at the vertices of an imaginary hexagon (**Fig. 2A'**). Three targets were presented in the right visual field (RVF) and three in the left visual field (LVF). Subjects performed the reaching task in total darkness under two different conditions. In both of them the patient and the control subjects pressed the central button for a variable control time (CT, 500-1000 ms), while fixating the central target. At the end of the CT one of the six peripheral targets appeared and the central one was extinguished. In the *foveal condition*, the subjects freely moved the eyes and then the hand to the target, within given hand reaction-time (RT; upper limit 3500 ms)

and movement-time (MT, upper limit 2500 ms). In the *extra-foveal condition* the central target stayed on and subjects moved the hand to the target while keeping fixation on it. The time limits imposed to different epochs were as in the *foveal condition*.

### *Isometric Reaching task*

A white target was presented first at the centre of wide screen computer monitor. By controlling an isometric joystick with one hand (**Fig. 2B**), subjects were required to move the cursor within it and keep it there for a variable control time (CT, 400-600 ms). At the end of the CT one of four peripheral visual targets was presented. The targets were located at the vertices of an imaginary square and subtended 20° of visual angle (**Fig. 2B'**). Two of them were presented in the RVF, two in the LVF. Subjects were requested to move the cursor from the central to the peripheral target and maintain the cursor there for a target-holding time (500 ms). Upper limits for RT and MT were 2000 ms and 2500 ms, respectively.

Similarly to the previous *reaching task* subjects performed the *Isometric Reaching task* under *foveal and extra-foveal* conditions. Across all tasks and conditions targets were presented in a pseudo-random sequence, until a minimum of 8 replications of each trial for each direction was collected.

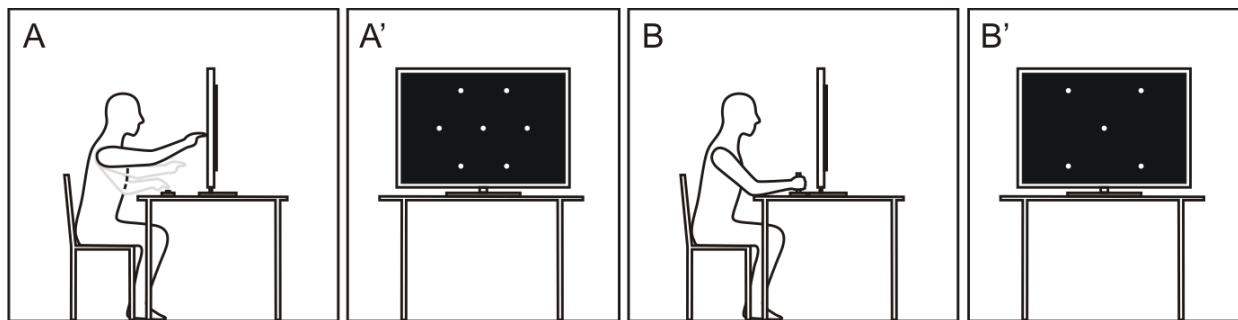


**Figure 2 – Experimental apparatus and tasks.** Lateral view of the experimental setup for the Reaching task (A) and for the Isometric Reaching task (B). Frontal view of the screen as viewed from the subject with all possible targets (white dots) presented during the conventional reaching (A') and during the isometric condition (B'). Subjects were instructed to fixate the central target, which disappeared at the end of the CT in the foveal condition.

In both tasks all the subjects performed the requested task with the head positioned on a chin rest in front of the screen. Eye movements were monitored through an infrared eye tracker (Arrington Research, Scottsdale AZ, USA) and sampled at 220 Hz. The isometric joystick (ATI Industrial Automation, Apex NC) measured the force applied with the hand in two dimensions, with a sampling frequency of 1000 Hz.

The patient was tested three days before surgery, and then three, twenty-one and 160 days after the operation.

## **Data processing and statistical analysis**

### *Reaction time*

The reaction time (RT) was defined as the time elapsing from target presentation to hand movement onset, as judged from the release of the central button in the reaching task, and from the velocity of the cursor in the *Isometric Reaching task*. In this latter case the onset of movement was considered as the first data point for which the cursor velocity exceeded a velocity threshold ( $v_T = 9.3$  deg/s) for at least 150 ms. The value of  $v_T$  was computed as the mean plus two standard deviations of the cursor velocity for all available data during a period of 200 ms centered at target onset.

### *Movement endpoints*

In the reaching task the hand movement endpoint was defined as the position where the finger touched the screen at the end of the movement. In the *Isometric Reaching task* it was defined as the farthest position from the center of the workspace reached by the cursor during each trial.

### *Field and hand-effect*

Two conditions have been classically distinguished in the reaching movements of OA patients: the field- and hand-effect (Perenin and Vighetto, 1988). A field effect is present when reaching movements are affected with either hand in the contralesional visual field. A hand effect can also be present, when the

contralesional hand misreaches in both the ipsi and contralesional fields.

In order to test if there was a global field effect on a given movement parameter (P), the following equation was used (Blangero et al, 2010):

$$\text{Field-effect index} = (cF - iF)_{CH} + (cF - iF)_{IH}$$

where *cF* and *iF* are the mean values of P in the contralesional and ipsilesional hemifield respectively, while *CH* and *IH* indicate that the values in parentheses refer to the contralesional and ipsilesional hand respectively.

In a similar manner, a hand-effect index was computed using the equation:

$$\text{Hand-effect index} = (cH - iH)_{CF} + (cH - iH)_{IF}$$

where *cH* and *iH* are the mean values of P obtained with the contralesional and ipsilesional hand respectively, and *CF* and *IF* indicate that the values in parentheses refer to the contralesional and ipsilesional field respectively.

### *Movement accuracy*

The movement accuracy was assessed by studying the constant errors (CE) of movement endpoint, representing the systematic deviation of the mean end-point from the target, as well as the spatial dispersion of the cursor trajectories across conditions and testing sessions.

To compute the spatial dispersion, all the trajectories in any given direction have been resampled to 20 equally spaced points and in each point the 95% confidence ellipse was calculated across all replications of movement. The mean area of all ellipses was used as the index of the spatial dispersion of the cursor path for each target direction.

### *Statistical comparisons*

To assess a statistically significant difference between the performance of the patient and that of the

control group a two-sided 95% prediction interval (PI) was calculated for the control subjects. A deficit was inferred if the patient's performance fell outside the controls' PI. A *p value*, corresponding to the probability that a normal control would obtain a more extreme result, was also computed using the modified form of *t-test* introduced by Crawford and Howell (Crawford and Garthwaite, 2012).



## RESULTS

The data presented in this manuscript refer to the patient's (FDL) performance tested three days before surgery, and twenty-one days after the operation for tumor removal in the right Superior Parietal Lobule (SPL). Hundred-sixty days after surgery, FDL performance under the task condition adopted was similar to controls, suggesting a significant recovery of function.

We will first describe the temporal aspect and then the spatial characteristics of the patient's performance across the different task.

### Temporal features of hand motor behavior

#### *Reaction Time*

First, the reaction-time (RT) of hand movement during different reach task conditions was studied and compared to that of controls. **Figure 3** shows that under isometric conditions reaches to extrafoveal targets displayed a significant elongation of the RT when performed with the contralesional hand (CH) toward targets located in the ipsilesional field (IF) and with the ipsilesional hand (IH) in the contralesional field (CF). No deficits were observed for reaches to foveated targets. Therefore, when considered separately for movements in each direction, the patient's RTs were not always significantly higher than those of controls. However, a tendency to an increase is evident and is probably responsible for the significance of the field effect, as it will be seen below.

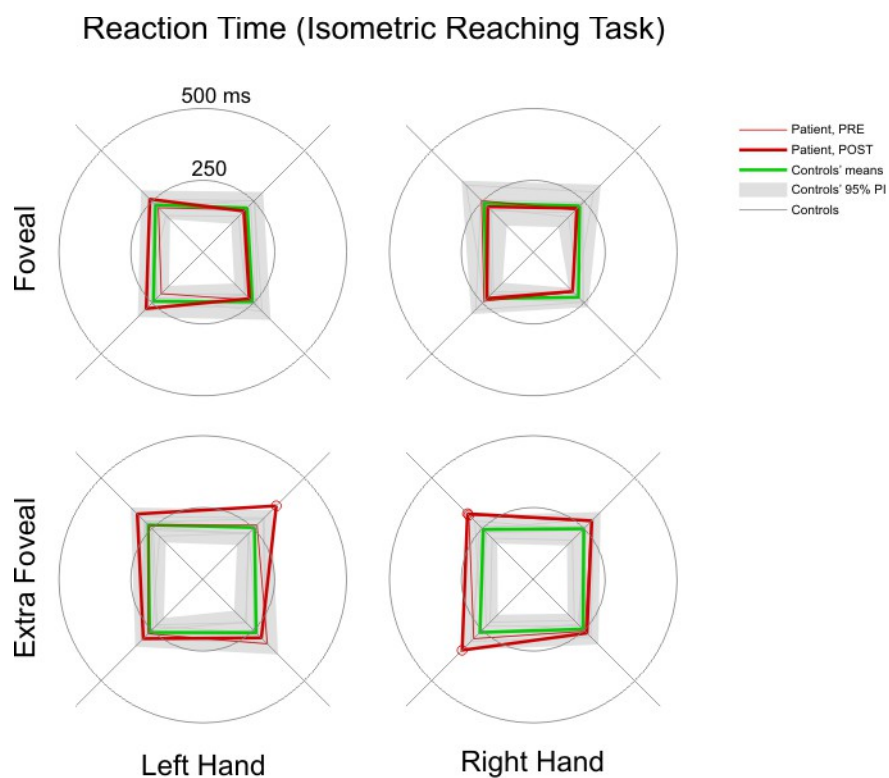


**Figure 3 - Reaction Time in the Isometric Reaching task.** Polar plots of the average RT values per direction of patient FDL before (thin red line) and after (thick red line) surgery, compared to controls (grey lines). The green line is the mean RT of all controls in each direction. The grey area represent the 95% PI of controls' values. The red circle indicates the movement direction for which a statistically significant difference in RT between the patient and controls was detected.

When comparing the patient's field-effect index for the RT to that of the control group (**Fig. 4A**), before surgery the patient did not present any deficit across conditions. On the contrary, post-surgery a significant elongation of the hand RT was observed while planning movement in the CH with both hands (field effect), also under isometric conditions, but not for conventional reaches to foveated targets. A hand-effect was not observed in any task or session (**Fig. 4B**). In fact, in the only condition where a significant difference between the patient's and controls' performance was observed (*Reaching task under foveal condition*) the hand-effect index had a negative value, indicating a significant elongation (relative to the controls) of the RT with the IH.

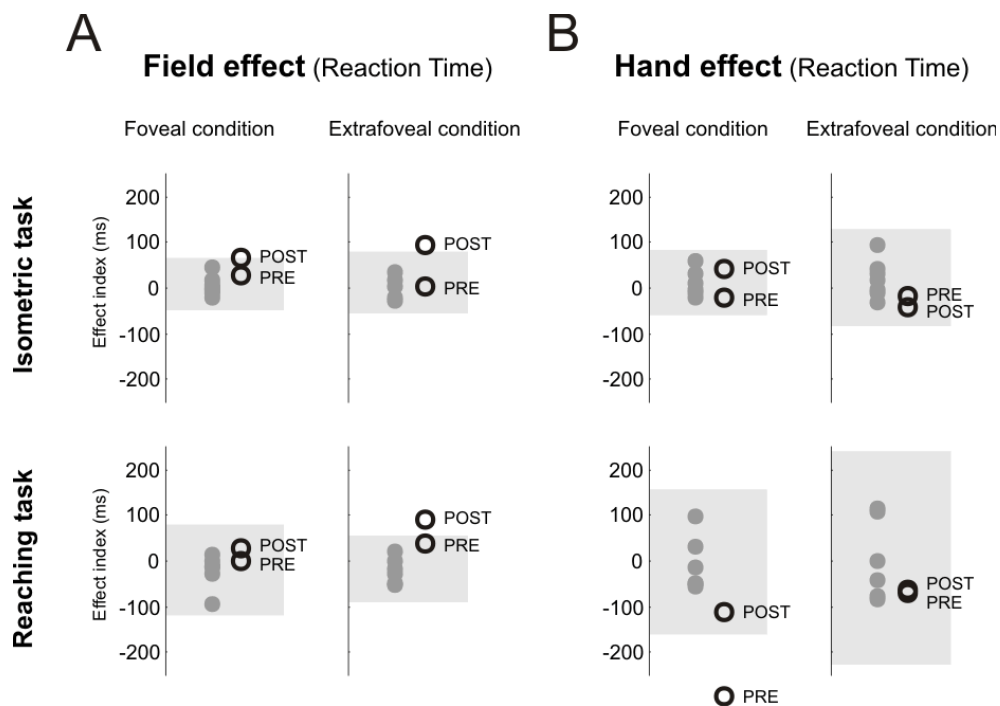


**Figure 4 - Field effect and Hand effect for the Reaction Time.** Field and hand effect index relative to the hand RT, for the two tasks in both fixation conditions. Markers indicate individual values of field- and hand-effect for the patient (open circles) and for control subjects (filled circles). The transparent gray rectangle represents the 95% PI of the controls' values. Positive values of the field effect index (panel A) indicate a longer RT in the contralesional hemifield as compared to the ipsilesional one. Positive values of the hand effect index (panel B) indicate a longer RT with the contralesional hand compared to the ipsilesional one. Notice that a field effect (panel A) was present for the patient after the surgery, in all conditions except for one (*Reaching task in the foveal condition*).

### *Movement time*

The patient's performance showed no statistical difference from controls concerning the total duration of the hand movement time across tasks and conditions.

### **Spatial parameters of hand motor behavior.**

The spatial aspects of movement of patient FDL were then analyzed by computing the constant error of the hand movement endpoints, as well as the spatial dispersion of the cursor trajectories, and by comparing them to controls.

### *Endpoint errors*

**Figure 5** shows the spatial distribution of the movement endpoints of FDL and of one control subject in the *Isometric* (**panel A**) and in the conventional *Reaching task* (**panel B**). Overall, it can be seen that the patient's performance differs from the control by a lower accuracy, due to a higher systematic deviation of the mean endpoint of its movements from the target location (constant error).

In the *Isometric Reaching task*, FDL made constant errors with the CH mostly in the CF, under both foveal and extrafoveal conditions. When using the IH, constant errors were smaller and were made in both hemifields. In the conventional reaching task, FDL misreached only to eccentric non-foveated targets. Constant errors were made with the CH in both hemifields, and with the IH mostly in the CF.

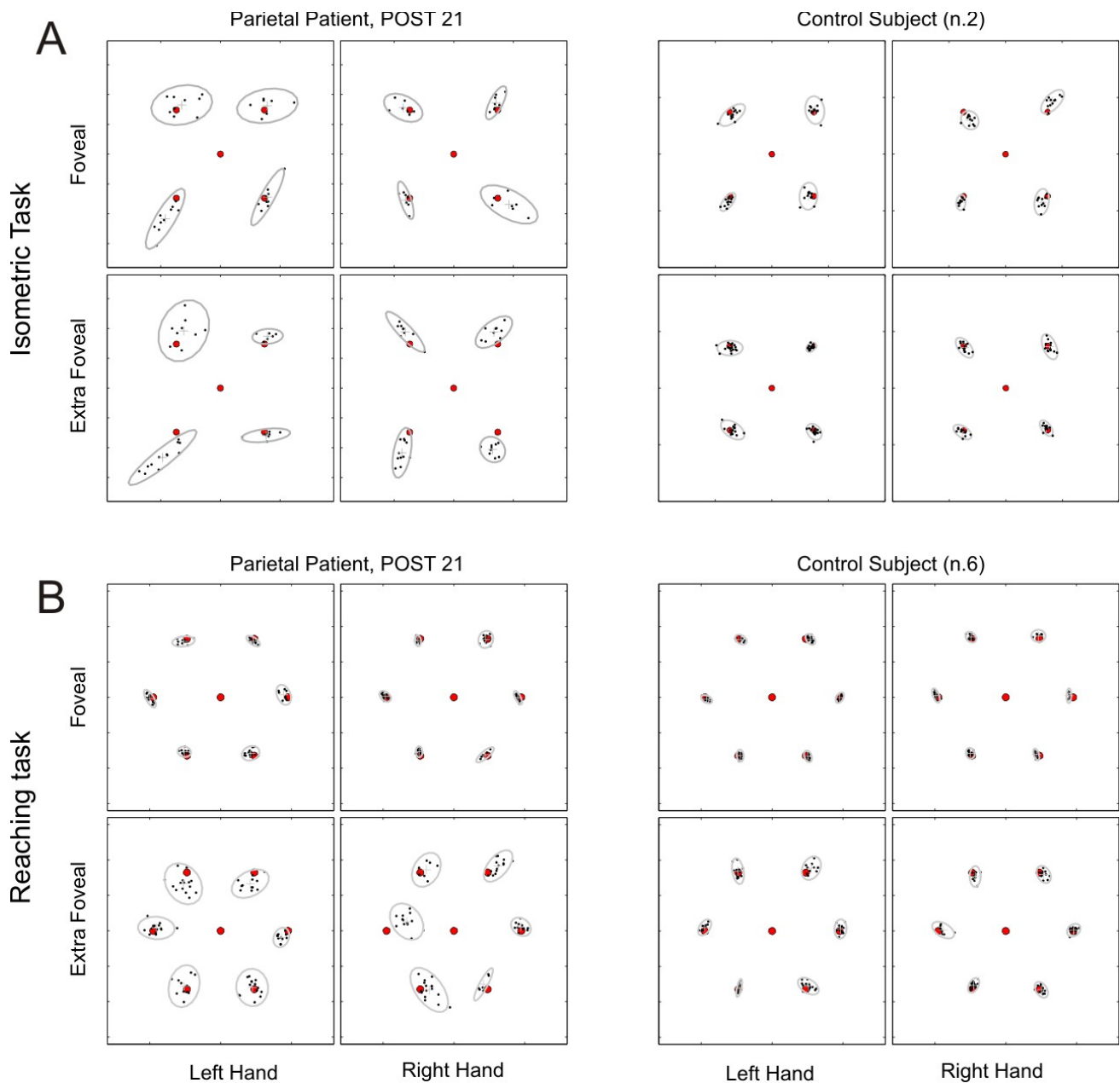


**Figure 5 - Movement endpoints.** Movement endpoints of patient FDL (left) tested 21 days after surgery and of one control subject (right) across conditions during the Isometric Reaching task (panel A) and the conventional reaching task (panel B). Each dot represents one movement endpoint. Red dots represent position and size of visual targets. Each gray cross is the average endpoint for a given target, and its distance from that target represents the constant error. Ellipses represent the 95% confidence region of the two-dimensional distribution of endpoints for each target.

### Constant error

The CE values for each direction in the *Isometric Reaching task* are shown in **Figure 6**, where a deficit is evident for movements with both hands towards the CF, especially toward targets located in the lower quadrant. Here, a statistically significant difference of CE between patient FDL and controls was observed across conditions and hands, indicating the presence of a field effect. When using the IH, the patient differed from controls also for movements toward extrafoveal targets located in the IF.



**Figure 6 - Constant Error in the isometric condition.** Constant error during the execution of the *Isometric Reaching task* for the patient (pre- and post-surgery, thin and thick red lines respectively) and for the control subjects (grey lines). Other conventions and symbols as in Figure 4. Across conditions and hands, the patient's CE in the contralesional (left) hemifield is statistically different compared to controls at least for one target, showing an evident field effect.

The quantitative analysis of the constant error was used to compute the field and hand-effect indices relative to this parameter across tasks and conditions. The results show a clear field effect in the *extra-foveal* conditions (**Fig. 7A**), for both conventional reaching (pre-surgery,  $p=0.002$  and post-surgery,  $p=0.02$ ), and isometric condition (pre-surgery,  $p=0.003$  and post-surgery,  $p<0.001$ ). When movement was directed toward faveated targets, a statistically significant field effect was present only in the *Isometric Reaching task* after surgery ( $p=0.02$ ), while it was not observed in the reaching task. On the contrary, a hand effect was not observed in any of the tasks and conditions (**Fig. 7B**).

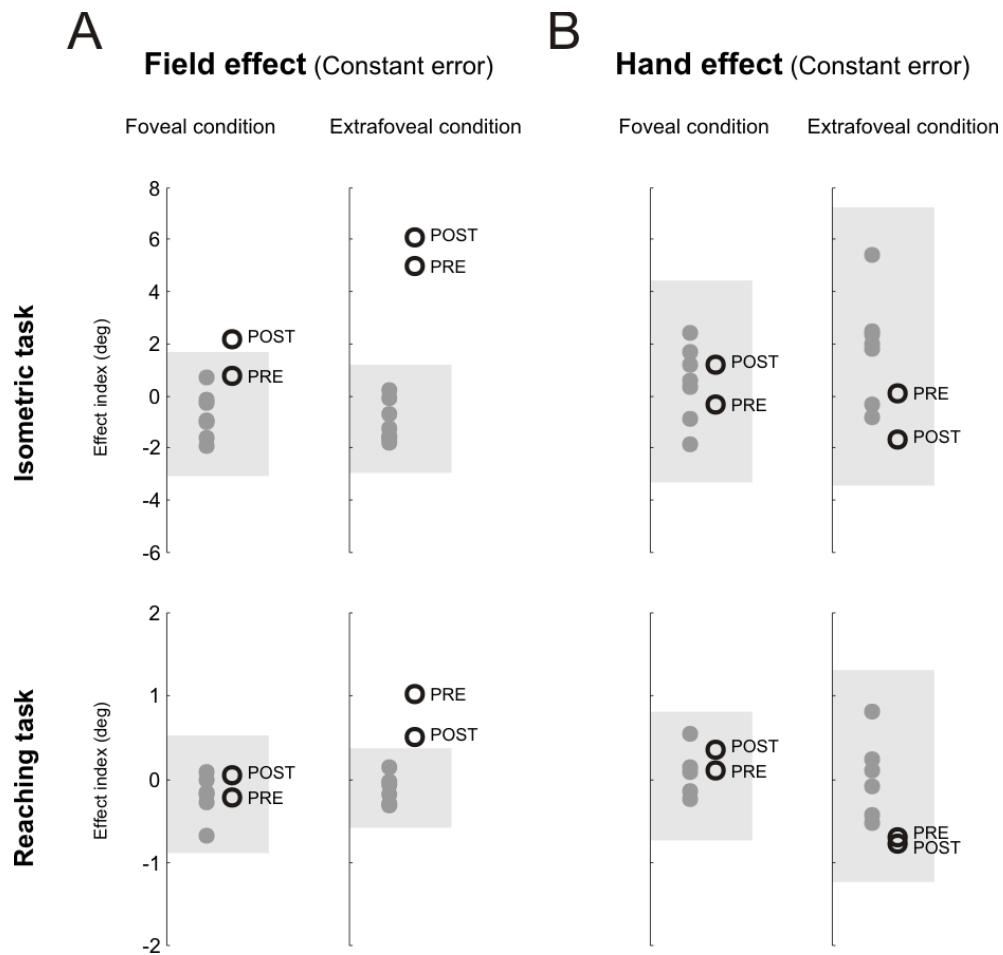


**Figure 7 - Field effect and Hand effect for the Constant Error.** Field- and Hand-effect indices relative to the CE for patient FDL (open circles) and control subjects (filled circles). Other conventions and symbols as in Figure 3. Note that in both tasks the patient shows a clear field effect when reaching to *extra-foveal* targets, while when moving toward *foveated targets* the field effect is present only after surgery in the isometric task.

### Spatial dispersion of cursor trajectories

The spatial dispersion of the parietal patient's cursor trajectories was analyzed across conditions and testing days and compared to that of normal controls.

For each movement direction and condition a two-dimensional region indicating the dispersion of the trajectories in space was calculated (see Methods). The results showed that the patient's movements were characterized by a high dispersion of the cursor trajectories as compared to controls (**Fig 8A**). It is worth stressing that this was true in all conditions. In fact, the difference between the patient's and controls' spatial dispersion was statistically significant in the *foveal condition* as well as in the *extra-foveal condition*, and in both tasks (**Fig 8B**).

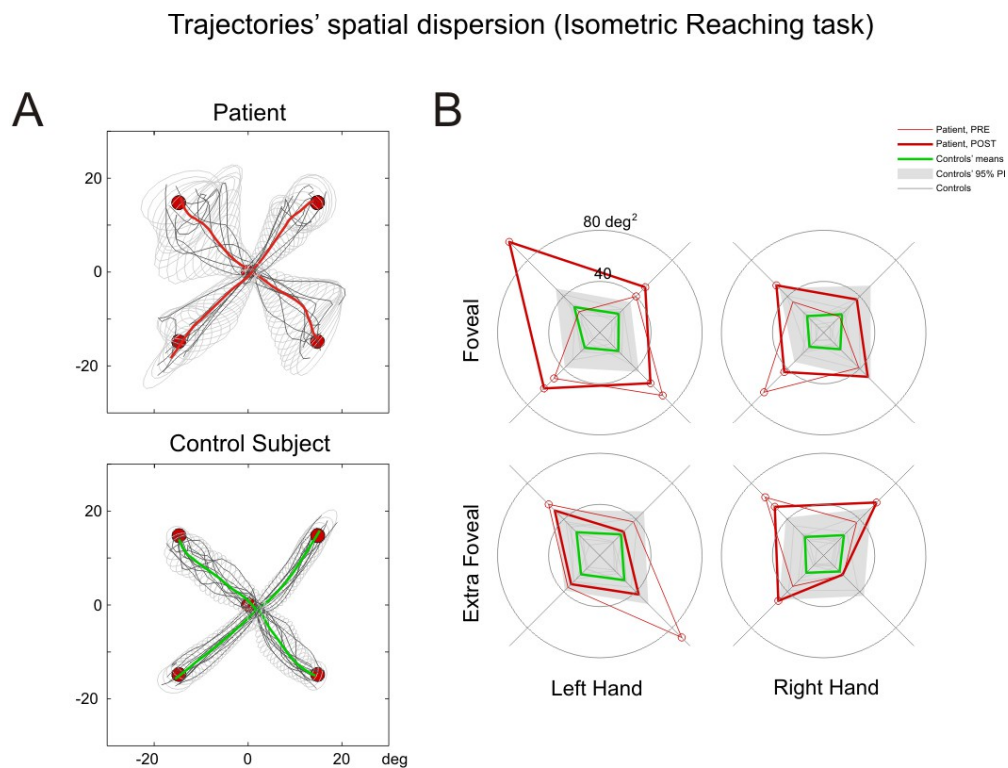


**Figure 8 - Spatial dispersion of hand movement trajectories in the isometric task.** *Panel A:* spatial dispersion of cursor trajectories for patient FDL and for one control subject. The patient's trajectories refer to data collected after the surgery, with the left hand, in foveal condition. Red dots represent the position and size of visual targets. Each grey line represents one trial's cursor trajectory. The thick red (FDL) and green (control) lines represent the average cursor trajectory across all replications for each target. Ellipses represent the 95% confidence area relative to each step of the resampled trajectories. *Panel B:* polar plots of the trajectories' mean spatial dispersion along the movement path. Conventions and symbols as in Figure 4.



## **Eye movements**

The study of eye movement of patient FDL revealed no significant alterations relative to control subjects. In fact, the reaction-time and movement time of saccades to peripheral visual targets were unaffected during both the conventional and the isometric reach task. Similarly, the trajectory of the eye from the central position to the targets were smooth, and their spatial dispersion did not differ significantly from controls, across all task conditions.

## DISCUSSION

### OA generalizes to isometric conditions

It is known since long time that lesion of the posterior parietal cortex results in OA (Balint 1909; Ratcliff and Davies-Jones, 1972), a disorder in which patients make inaccurate reaching movement mostly to extrafoveal targets, rarely to foveated targets. This deficit occurs in patients free of primary sensory, motor or attention disorders (Balint 1909; Ratcliff and Davies-Jones, 1972; Perenin and Vighetto, 1988; Striemer et al., 2009). OA for reaches in both central and peripheral vision has been documented in a few cases (Rondot et al, 1977; Perenin and Vighetto, 1988; Buxbaum and Coslett, 1998; Rossetti et al., 2003).

In all cases so far reported in the literature, OA has been assessed by analyzing the temporal and spatial aspects of reaches requiring the physical displacement of the arm from a starting position to a visual target. It is widely assumed that such movements occurs thanks to a remapping mechanism that aligns visual information about target location and proprioceptive signals about arm position and geometry into dynamic reference frames, whose nature depends on the context in which reaches are made (Battaglia-Mayer et al., 2003; McGuire and Sabes 2009).

Here we show for the first time that OA after parietal lesion affects the process of coordinate transformation not only for conventional reaches, but also when no physical displacement of the arm is required and movement occurs under isometric condition. In this task, a force of desired amplitude and direction is exerted as to move a cursor from a central position on visual targets located on the display, thus requiring the combination of target location signals with information from force receptors. Furthermore, contrary to conventional reaching movements, under isometric conditions the endpoint of eye movement does not coincide with that of hand movement. This suggest that parietal cortex contains simultaneous representations of different reference frame where sensory signals can be combined in an optimal fashion (Battaglia-Mayer et al 2003; McGuire and Sabes 2009) rather than the representation of reaching in a unique (Batista et al., 1999) reference frame. Under these assumption, it is not surprising that OA generalizes to

isometric conditions.

### **OA emerges when eye and hand positions are disjoint**

There is a vast literature showing that OA is by far more common when patients reach to target located in the periphery rather than in the center of the visual field. When making conventional reaches, patient FDL made errors when he was not allowed to foveate to the target, thus the final eye and hand position were dissociated, but not for reaches to foveated targets, on which the final eye and hand position were spatially coincident. On contrary, under isometric condition, FDL misreached not only to peripheral targets, but also to targets in central vision. Also in this case the position of the eye and that of the hand did not coincide in space, due to the different locations of the visual targets, which were presented on the screen, and of the hand acting on the isometric manipulandum. This suggests that parietal cortex is essential for combining position signals coming from different effectors, such as the eye and the hand, as to provide a central representation of their relative position. This can be achieved thanks to the global tuning field of parietal neurons (Battaglia-Mayer et al., 2000; Mascaro et al., 2003) where eye and hand position signals are represented within a common directional space whose size determines the limit of the combinatorial properties of parietal neurons. The breakdown of this combinatorial mechanisms can lead to OA, as hypothesized in previous studies (Battaglia-Mayer et al., 2000; Battaglia-Mayer and Caminiti, 2002).

### **OA affects hand trajectory formation**

A profound effect of parietal lesion was observed on hand trajectories. These were affected mostly when hand movement were made in the isometric task, and across all task conditions, therefore during movement to foveal and extrafoveal targets, regardless of whether these were performed with the ipsilateral or contralateral hand and to targets in the ipsilesional or contralesional space. This defect consisted in a significantly higher spatial dispersion, relative to controls, of the cursor trajectories resulting from the forces applied to the joystick. To our knowledge this is the first time that this deficit is assessed in a quantitative

fashion in OA patients and suggest a critical role of parietal cortex in hand trajectory formation.

### **OA affects the timing of planning, not execution of hand movements**

Patient FDL made reach errors in time, since a significant elongation of the time required for planning hand movement was observed for both hands in the contralesional left space. This field effect (Perenin and Vighetto, 1988) was observed under isometric conditions, but not for conventional reaches to foveated targets. As for the accuracy errors, this deficit is observed when planning reaches characterized by disjoint endpoint of eye and hand movement. No elongation of the hand movement time was observed in this patient, indicating that the parietal lesion affected planning and not execution of movement.

### **Conclusions**

Optic Ataxia in parietal patients is characterized by defective hand movement to visual targets, especially in the periphery of the visual field. We tested a patient with OA when he performed conventional reaches and when he exerted forces in different directions on an isometric joystick, as to move a visual cursor to the same visual targets. We found that OA generalizes to isometric conditions. Here, dispersion of hand trajectories and reaching errors were found not only on peripheral targets, but also for targets located in central vision. Under isometric condition, even if the targets are in foveal vision, the endpoints of eye and hand movement remain dissociated, as for conventional reaches to eccentric target. Thus, OA emerges only when the endpoints of eye and hand movement are disjoint, regardless of whether targets are located in central or peripheral vision. This novel finding add a new dimension to understanding this baffling syndrome. The results of this case report also suggests that lesion of PPC affects sensory-motor transformations not only when they require a physical displacement of the hand, but also when visual signals from target location need to be aligned with information from force receptors.

## REFERENCES

- Andersen RA, Brotchie PR, Mazzoni P (1992) Evidence for the lateral intraparietal area as the parietal eye field. *Curr Opin Neurobiol.* 2:840-846.
- Archambault PS, Caminiti R, Battaglia-Mayer A (2009) Cortical mechanisms for online control of hand movement trajectory: the role of the posterior parietal cortex. *Cereb Cortex.* 19:2848-2864.
- Archambault PS, Ferrari-Toniolo S, Battaglia-Mayer A (2011) Online Control of hand trajectory and evolution of motor intention in the parietofrontal system. *J Neurosci.* 31:742-752.
- Bakola S, Gamberini M, Passarelli L, Fattori P, Galletti C (2010) Cortical Connections of Parietal Field PEc in the Macaque: Linking Vision and Somatic Sensation for the Control of Limb Action. *Cereb Cortex.* 20:2592-2604
- Balint R (1909) Seelenlähmung des "Schauens", optische Ataxia, räumliche Störung der Aufmerksamkeit. *Monatsschrift für Psychiatrie und Neurologie.* 25:51-81.
- Bard C, Turrell Y, Fleury M, Teasdale N, Lamarre Y, Martin O (1999) Deafferentation and pointing with visual double-step perturbations. *Exp Brain Res.* 125:410-416.
- Batista AP, Buneo CA, Snyder LH, Andersen RA (1999) Reach plans in eye-centered coordinates. *Science* 285:257-260.
- Battaglia-Mayer A, Ferraina S, Mitsuda T, Marconi B, Genovesio A, Onorati P, Lacquaniti F, Caminiti R (2000) Early coding of reaching in the parieto-occipital cortex. *J Neurophysiol.* 83(4):2374-2391.
- Battaglia-Mayer A, Ferraina S, Genovesio A, Marconi B, Squatrito S, Lacquaniti L, Caminiti R (2001) Eye-hand coordination during reaching. II. An analysis of the relationships between visuomanual signals in parietal cortex and parieto-frontal association projections. *Cereb Cortex.* 11:528-544.
- Battaglia-Mayer A and Caminiti R (2002) Optic ataxia as result of the breakdown of the global tuning fields of parietal neurons. *Brain.* 125:1-13.

- Battaglia-Mayer A, Caminiti R, Lacquaniti F, Zago M (2003) Multiple levels of representation of reaching in the parieto-frontal network. *Cereb Cortex*. 13:1009-1022.
- Battaglia-Mayer A, Archambault PS, Caminiti R (2006) The cortical network for eye–hand coordination and its relevance to understanding motor disorders of parietal patients. *Neuropsychol* 44:2607–2620.
- Battaglia-Mayer A, Ferrari-Toniolo S, Visco-Comandini F, Archambault PS, Saberi-Moghadam S, Caminiti R (2012) Impairment of Online Control of Hand and Eye Movements in a Monkey Model of Optic Ataxia. *Cereb Cortex. online*, doi:10.1093/cercor/bhs250.
- Baylis GC, Baylis LL (2011) Visually misguided reaching in Balint’s syndrome. *Neuropsychologia*. 39:865-875.
- Bisley JW, and Goldberg ME (2010) Attention, intention, and priority in the parietal lobe. *Annu Rev Neurosci*. 33:1–21.
- Blangero A, Ota H, Rossetti Y, Fujii T, Ohtake H, Tabuchi M, Vighetto A, Yamadori A, Vindras P, and Pisella L (2010) Systematic retinotopic reaching error vectors in unilateral optic ataxia. *Cortex* 46:77–93.
- Blouin J, Teasdale N, Bard C, Fleury M (1995) Control of rapid arm movements when target position is altered during saccadic suppression. *J Mot Behav*. 27:114-122.
- Buxbaum LJ and Coslett HB (1998) Spatio-motor representations in reaching: Evidence for subtypes of optic ataxia. *Cogn Neuropsychol*. 15:279–312.
- Buxbaum LJ, Ferraro MK, Veramonti T, Farne A, Whyte J, Ladavas E, Frassinetti F, Coslett HB (2004) Hemispatial neglect: subtypes, neuroanatomy, and disability. *Neurology*. 62:749–756
- Caminiti R, Chafee MV, Battaglia-Mayer A, Averbeck B, Crowe DA, Georgopoulos AP (2010) Understanding the parietal lobe syndrome from a neurophysiological and evolutionary perspective. *Eur J Neurosci*. 31:2320–2340.
- Carey DP (2000) Eye-hand coordination: eye to hand or hand to eye? *Curr Biol*. 10:416–419.
- Carlton LG (1981) Processing visual feedback information for movement control. *J Exp Psychol Hum Percept Perform*. 7:1019-1030.
- Crawford JR & Garthwaite PH (2012) Single case research in neuropsychology: A comparison of five forms of

- t-test for comparing a case to controls. *Cortex* 48:1009-1016.
- d'Avella A, Portone A, Lacquaniti F (2011) Superposition and modulation of muscle synergies for reaching in response to a change in target location. *J Neurophysiol.* 106:2796-2812.
- De Renzi E (1982) Disorders of Space Exploration and Cognition. *Wiley, New York*
- Desmurget M, Epstein CM, Turner RS, Prablanc C, Alexander GE, Grafton ST (1999) Role of the posterior parietal cortex in updating reaching movements to a visual target. *Nat Neurosci.* 2:563-567.
- Desmurget M, Grafton S (2000) Forward modelling allows feedback control for fast reaching movements. *Trends Cogn Neurosci.* 411:423-431.
- Diedrichsen J, Hashambhoy Y, Rane T, Shadmehr R (2005) Neural correlates of reach errors. *J Neurosci.* 25:9919-9931.
- Filimon F (2010) Human cortical control of hand movement: Parieto-frontal networks for reaching, grasping, and pointing. *Neuroscientist.* 16:388-407.
- Fogassi L, Ferrari PF, Gesierich B, Rozzi S, Chersi F and Rizzolatti G (2005) Parietal Lobe: from Action Organization to Intention Understanding. *Science.* 308:662-7.
- Gaveau V, Pélisson D, Blanghero A, Urquizar C, Prablanc C, Vighetto A, Pisella L (2008) Saccade control and eye-hand coordination in optic ataxia. *Neuropsychologia.* 46:475-486.
- Georgopoulos AP, Kalaska JF, Massey JT (1981) Spatial trajectories and reaction times of aimed movements: effects of practice, uncertainty and change in target location. *J Neurophysiol.* 46:725-743.
- Georgopoulos AP, Kalaska JF, Caminiti R, Massey JT (1983) Interruption of motor cortical discharge subserving aimed arm movements. *Exp Brain Res.* 49:327-340.
- Gielen CCAM, van den Heuvel PJM, van Gisbergen JAM (1984) Coordination of fast and arm movements in a tracking task. *Exp Brain Res.* 56:154-161.
- Gold JI and Shadlen MN (2007) The neural basis of decision making. *Annu. Rev. Neurosci.* 30:535–574.
- Gréa H, Pisella L, Rossetti Y, Desmurget M, Tilikete C, Grafton S, Prablanc C, Vighetto A (2002) A lesion of the posterior parietal cortex disrupts on-line adjustments during aiming movements. *Neuropsychologia.*

40:2471–2480.

Hécaen H and de Ajuriaguerra J (1954) Balint's syndrome (Psychic paralysis of visual fixation and its minor forms). *Brain*. 77:373–400 .

Herman R, Herman R, Maulucci R (1981) Visually triggered eye-arm movements in man. *Exp Brain Res*. 42:392-398.

Johnson H, Haggard P (2005) Motor awareness without perceptual awareness. *Neuropsychologia*. 43:227-237.

Johnson PB, Ferraina S, Bianchi L, Caminiti R (1996) Cortical networks for visual reaching: Physiological and anatomical organization of frontal and parietal lobe arm regions. *Cereb Cortex*. 6:102-119.

Kalaska JF, Scott SH, Cisek P, Sergio LE (1997) Cortical control of reaching movements. *Curr Opin Neurobiol*. 7:849–859.

Lacquaniti F, Guigon E, Bianchi L, Johnson PB, Ferraina S, Caminiti R (1995) Representing spatial information for limb movement: The role of area 5 in the monkey. *Cereb Cortex*. 5:391:409.

Levy I, Schluppeck D, Heeger DJ, Glimcher PW (2007) Specificity of human cortical areas for reaches and saccades. *J Neurosci*. 27:4687–4696.

Marconi B, Genovesio A, Battaglia-Mayer A, Ferraina S, Squatrito S, Molinari M, Lacquaniti F, Caminiti R (2001) Eye-hand coordination during reaching. I. Anatomical relationships between parietal and frontal cortex. *Cereb Cortex*. 11:513-527.

Mascaro M, Battaglia-Mayer A, Nasi L, Amit D, Caminiti R (2003) The eye and the hand: neural mechanisms and network models for oculomanual coordination. *Cereb Cortex*. 13:1276–1286.

McGuire LM, Sabes PN (2009) Sensory transformations and the use of multiple reference frames for reach planning. *Nat Neurosci*. 12:1056–1061.

Morasso P (1981) Spatial control of arm movement. *Exp Brain Res*. 42:223-227.

Neggers SFW, Bekkering H (2002) Coordinated control of eye and hand movements in dynamic reaching. *Hum Mov Sci*. 21:349-376.



- Pelisson D, Prablanc C, Goodale MA, Jeannerod M (1986) Visual control of reaching movements without vision of the limb. II Evidence of fast unconscious processes correcting the trajectory of the hand to the final position of a double-step stimulus. *Exp Brain Res.* 62:303-311.
- Perenin MT, Vighetto A (1988) Optic Ataxia: a specific disruption in visuomotor mechanisms. I. Different aspects of the deficit in reaching for objects. *Brain.* 111:643-674.
- Pierrot-Deseilligny C, Milea D, Muri RM (2004) Eye movement control by the cerebral cortex. *Curr Opin Neurol.* 17:17–25.
- Pisella L, Gréa H, Tilikete C, Vighetto A, Desmurget M, Rode G, Boisson D, Rossetti Y (2000) An "automatic pilot" for the hand in human posterior parietal cortex: toward reinterpreting optic ataxia. *Nat Neurosci.* 3:729–736.
- Prablanc C, Echallier JF, Komilis E, Jeannerod M (1979) Optimal response of eye and hand motor systems in pointing at visual target. I. Spatio-temporal Characteristics of eye and hand movements and their relationships when varying the amount of visual information. *Biol Cybernetics.* 35:113-124.
- Ratcliff G and Davies-Jones GAB (1972) Defective visual localization in focal brain wounds. *Brain,* 95(1):49-60
- Rondot P, Derecondo J and Ribadeau Dumas JL (1977) Visuomotor ataxia. *Brain,* 100:355-376.
- Rossetti Y, Pisella L and Vighetto A (2003) Optic ataxia revisited: visually guided action versus immediate visuomotor control. *Exp. Brain Res.* 153:171–179.
- Sarlegna FR, Gauthier GM, Bourdin C, Vercher JL, Blouin J (2006) Internally driven control of reaching movements: a study on a proprioceptively deafferented subject. *Brain Res Bull.* 69:404-415.
- Shadmur R, Mussa-Ivaldi FA (1994) Adaptive representation of dynamics during learning of a motor task. *J Neurosci.* 14:3208-3224.
- Snyder LH, Calton JL, Dickinson AR, Lawrence BM (2009) Eye-hand coordination: saccades are faster when accompanied by a coordinated arm movement. *J Neurophysiol.* 87:2279–2286.
- Soechting JF, Lacquaniti F (1983) Modification of trajectory of a pointing movement in response to a change in target location. *J Neurophysiol.* 49:548-564.

- Squatrito S, Raffi M, Maioli, MG, Battaglia-Mayer A (2001) Visual motion responses of neurons in the caudal area PE of macaque monkey. *J Neurosci.* 21(4):RC130.
- Striemer C, Blangero A, Rossetti Y, Boisson D, Rode G, Vighetto A, Pisella L, Danckert J (2007) Deficits in peripheral visual attention in patients with optic ataxia. *Neuroreport*, 18(11):1171–1175.
- van Beers RJ (2007) The sources of variability in saccadic eye movements. *J Neurosci.* 27:8757–8770.
- van Opstal AJ, van Gisbergen JAM (1989) Scatter in the metrics of saccades and properties of the collicular motor map. *Vision Res.* 29:1183-1196.
- Wakana S, Jiang H, Nagae-Poetscher LM, van Zijl PC, Mori S (2004) Fiber tract-based atlas of human white matter anatomy. *Radiology.* 230(1):77-87.
- Yasargil MG (1994) *Microneurosurgery, Vol IVA. Stuttgart: Georg Thieme Verlag*
- Zar JH (1996) *Biostatistical Analysis. Prentice-Hall International, INC, Upper Saddle River, N.J.*